Mixed and Galerkin Finite Element Approximation of Flow in a Linear Viscoelastic Porous Medium

Eduard Rohan[*], Simon Shaw[†], Mary F Wheeler[‡] and John R Whiteman[§]

February 1, 2013

Contents

[*]Faculty of Applied Sciences, University of West Bohemia in Pilsen, Univerzitni 8, 30614 Plzen, Czech Republic. rohan@kme.zcu.cz.

[†]✉ Institute of Computational Mathematics (BICOM), Brunel University, Uxbridge, UB8 3PH, England. simon.shaw@brunel.ac.uk.

[‡]Center for Subsurface Modeling (CSM), Institute for Computational Engineering and Sciences (ICES), Department of Aerospace Engineering and Engineering Mechanics, Department of Petroleum Engineering and Geosystems Engineering, University of Texas at Austin, Austin, Texas, USA. mfw@ices.utexas.edu.

[§]Institute of Computational Mathematics (BICOM), Brunel University, Uxbridge, UB8 3PH, England. john.whiteman@brunel.ac.uk.

Abstract

We propose two fully discrete mixed and Galerkin finite element approximations to a system of equations describing the slow flow of a slightly compressible single phase fluid in a viscoelastic porous medium. One of our schemes is the natural one for the backward Euler time discretization but, due to the viscoelasticity, seems to be stable only for small enough time steps. The other scheme contains a lagged term in the viscous stress and pressure evolution equations and this is enough to prove unconditional stability. For this lagged scheme we prove an optimal order *a priori* error estimate under ideal regularity assumptions and demonstrate the convergence rates by using a model problem with a manufactured solution. The model and numerical scheme that we present are a natural extension to 'poroviscoelasticity' of the poroelasticity equations and scheme studied by Philips & Wheeler in (for example) *Comput. Geosci.* **11**, 145–158, 2007 although — importantly — their algorithms and codes would need only minor modifications in order to include the viscous effects. The equations and algorithms presented here have application to oil reservoir simulations and also to the condition of *hydrocephalus* — 'water on the brain'. An illustrative example is given demonstrating that even small viscoelastic effects can produce noticeable differences in long-time response. To the best of our knowledge this is the first time a mixed and Galerkin scheme has been analysed and implemented for viscoelastic porous media.

Keywords: porous media, viscoelasticity, finite element method, error estimates, time stepping, geoengineering, bioengineering.

Sub. class: 65M15, 74D05, 76S05, 74L15

1 Introduction and motivation

In this article we consider an extension to the equations of poroelasticity by modelling the flow of a slightly compressible single phase fluid in a viscoelastic porous medium. The constitutive equations therefore allow for the presence of viscoelastic relaxation effects in the porous media (but not the fluid). Fully discrete numerical schemes are derived based on a lagged and non-lagged backward Euler time stepping method applied to a mixed and Galerkin finite element spatial discretization. We show that the lagged scheme is unconditionally stable and give an optimal *a priori* error bound for it. Furthermore, this scheme is practical and useful in the sense that it can be easily implemented in existing poroelasticity software because the coupling between the viscous stresses and pressures and the elasticity and flow equations is 'lagged' by one time step. The required additional coding therefore takes the form of extra 'right hand side loads' together with some updating subroutines for the viscoelastic *internal variables*, but the solver and assembly engines remain intact. This idea of lagging has been used before for nonlinearly viscoelastic diffusion problems in [3, 24] but, of course, is not new. Lagging in numerical schemes is discussed more widely by Lowrie in [14].

This work was originally motivated by geomechanics applications but during its development we have become aware of its potential relevance to the modelling of cerebrospinal fluid flow and its relation to the condition of *hydrocephalus*. To the best of our knowledge this is the first time a mixed and Galerkin scheme has been analysed and implemented for viscoelastic porous media.

1.1 Geomechanics

Reservoir simulators are built by computationally solving partial differential equations that employ Darcy's law to approximate the flow through porous media. The oil reservoirs can be anywhere between 300 m to 10 km below the earth's surface in the lithosphere. At the simplest level of modelling the lithosphere (the porous medium) can be considered as pefectly rigid but, in practice, it is more accurately modelled as being either elastic or viscoelastic as in, for example, [2, Chap. 2] and [18, 6, 31]. The point made by Lakes in [12, § 7.4.1] is that although at room temperatures rock is not in general a 'lossy' medium, at the elevated temperatures in the Earth's interior the viscoelastic loss tangents can be significant. Also in [12, § 8.3.1], an explanation of viscoelastic behaviour of porous media even at cooler temperatures is given based on the time and frequency dependent drag forces from the stress-induced fluid flow.

Recently Philips and Wheeler in [20, 21, 22] and then Wheeler and Gai in [32] described, discretized and analysed a poroelasticity model in which the porous rock was allowed to behave linear elastically (see for example [7, 5]). Rohan *et al.* in [25] then followed by using homogenisation techniques to extend that poroelasticity model by including linear viscoelastic effects. Under the assumption of slow fluid flow, that model — considered below — is able to simulate relaxation and creep behaviour, as well capture damping and frequency dependent behaviour (see the interesting article [4] for an idea of the importance of viscoelastic damping in geology).

1.2 Cerebrospinal fluid (CSF) flow

Our original connection to this potential application came through exposure to the work that now appears in [9]. Here the flow of CSF through the ventricles of an elastic-sponge-like brain is modelled using essentially the same equations of poroelasticity as touched on above. The work in [9] follows on from the developments presented in [28, 34] and is related to the studies in [26, 27, 33]. The last authors note that brain tissue is in general viscoelastic as described in, for example, [30, 17, 29, 19] and [12, § 7.5.7] and this provides the connection to the work presented in [25] and below.

We should also mention that the model in [9] allows for nonlinear compression-dependent effects, and also that [35] extends the model to finite strain hyperelasticity.

1.3 Poro-visco-elasticity

Although the idea of viscoelastic porous media modelling and numerics is not new (see also [8] and the comprehensive [15] as well as the those above) we believe that this paper

is the first to present it in a mixed and Galerkin framework.

The viscoelasticity of the porous media is introduced into the poroelasticity model by using a stress relaxation ODE (ordinary differential equation) for an 'internal stress variable' rather than the using the equivalent (when a Prony series relaxation function is assumed) notion of a 'hereditary integral'. This extension of Hooke's law to linear viscoelasticity is classical and very well documented in the literature (see, for example, [11, 10]). What is not so obvious is how the viscoelasticity of the skeleton influences the flow equation for pressure. To reveal this mechanism Rohan *et al.* in [25] used homogenization arguments to derive the governing equations that appear below.

Although for the reasons touched on earlier this viscoelastic porous media model is useful in its own right, in another respect it serves (at least mathematically) as a starting point for adding other forms of internal variable equations. These can represent more complicated behaviour such as, for example, plasticity as formulated in [1]. We hope to return to these extensions at a later time as well as to other important topics such as the *thermoporoelasticity* model described in [13].

We now move on to describe the model with which we shall be concerned. This will be followed in Section 3 with the numerical scheme; in Section 4 with a derivation of error bounds; in Section 5 with an illustration of these bounds and in Section 6 with a more practically-oriented demonstration of the model. We finish in Section 7 with some concluding remarks.

In isotropic linear elasticity theory in $\mathbb{R}^d$ the symmetric stress tensor, $\underline{\boldsymbol{\sigma}} = (\sigma_{ij})_{i,j=1}^d$ is related to the strain tensor, $\underline{\boldsymbol{\varepsilon}} = (\varepsilon_{ij})_{i,j=1}^d$ through the constitutive law,

$$\underline{\boldsymbol{\sigma}} = \underline{\boldsymbol{D}}\underline{\boldsymbol{\varepsilon}} \qquad \text{or} \qquad \sigma_{ij} = \lambda \varepsilon_{kk}(\boldsymbol{u})\delta_{ij} + 2\mu\varepsilon_{ij}(\boldsymbol{u})$$

where $\varepsilon_{ij}(\boldsymbol{u}) := \frac{1}{2}(u_{i,j}+u_{j,i})$ and with $\boldsymbol{u} = (u_i)_{i=1}^d$ the displacement and λ, μ the Lamé constants. Unless explicitly stated otherwise the summation convention is in force throughout and we usually suppress $\boldsymbol{x}$ dependence to enhance readability. Note that $\underline{\boldsymbol{D}}$ is positive definite on the symmetric second-order tensors and also that we are writing tensors of order one ('vectors') in bold and tensors of order two or four in bold underline.

The simplest way of including viscoelastic effects such as stress relaxation and creep is to introduce a history functional into the constitutive law (see e.g. [10],[11]). For this we introduce the *stress relaxation function* $\varphi(t) = \varphi_0 + \varphi_1 e^{-t/\tau}$, for constants $\varphi_0 > 0$, $\varphi_1 \geqslant 0$ and $\tau > 0$ such that $\varphi(0) = 1$, and write the stress as,

$$\underline{\boldsymbol{\sigma}} = \underline{\boldsymbol{D}}\underline{\boldsymbol{\varepsilon}}(\boldsymbol{u}(t)) + \int_0^t \dot{\varphi}(t-s)\underline{\boldsymbol{D}}\underline{\boldsymbol{\varepsilon}}(\boldsymbol{u}(s))\,ds$$

where, here and below, the overdot signifies partial differentiation with respect to the (time) argument. It is a fundamental observation that with $\psi_0 = 1/\varphi_0$ and $\psi_1 = \varphi_1/\varphi_0$ this relationship can be inverted to give,

$$\underline{\boldsymbol{D}}\underline{\boldsymbol{\varepsilon}}(\boldsymbol{u}(t)) = \underline{\boldsymbol{\sigma}}(t) + \int_0^t \dot{\psi}(t-s)\underline{\boldsymbol{\sigma}}(t)\,ds$$

where $\psi(t) = \psi_0 - \psi_1 e^{-\varphi_0 t/\tau}$ is the *creep function*. Furthermore, noting that $\dot{\varphi}(t-s) = -\tau^{-1}\varphi_1 \exp(-(t-s)/\tau)$ we define the *internal stress variable*

$$\underline{\boldsymbol{\sigma}}^*(t) := \int_0^t \frac{\varphi_1}{\tau} e^{-(t-s)/\tau}\underline{\boldsymbol{D}}\underline{\boldsymbol{\varepsilon}}(\boldsymbol{u}(s))\,ds \tag{1}$$

and get

$$\tau\dot{\underline{\boldsymbol{\sigma}}}^* + \underline{\boldsymbol{\sigma}}^* = \varphi_1 \underline{\boldsymbol{D}}\underline{\boldsymbol{\varepsilon}}(\boldsymbol{u}) \qquad \text{subject to} \qquad \underline{\boldsymbol{\sigma}}^*(0) = \underline{\mathbf{0}}.$$

With this we can write $\underline{\boldsymbol{\sigma}}(t) = \underline{\boldsymbol{D}}\underline{\boldsymbol{\varepsilon}}(\boldsymbol{u}(t)) - \underline{\boldsymbol{\sigma}}^*(t)$ and thereby remove the explicit appearance of the displacement history.

Now letting p denote the pressure field and assuming that p and $\boldsymbol{u}$ are zero at $t = 0$ we appeal to the simplest form of the model presented by Rohan *et al.* in [25] and, on borrowing terminology from poroelasticity, find that the *total stress*, $\tilde{\sigma}_{ij} := \sigma_{ij} - \alpha\delta_{ij}p$, is given by,

$$\tilde{\sigma}_{ij} = \int_0^t \varphi(t-s) D_{ijkl} \frac{\partial}{\partial s} \varepsilon_{kl}(\boldsymbol{u}(s))\, ds - (\beta_{ij} + \phi\delta_{ij})p \tag{2}$$

where $\beta_{ij} + \phi\delta_{ij}$ are the Biot stress coefficients with $\underline{\boldsymbol{\beta}}$ symmetric and $\phi > 0$ the volume fraction of the fluid part. We will make the simplifying assumption that $\beta_{ij} = \beta\delta_{ij}$ for a positive real number β and then after integration by parts we obtain

$$\tilde{\sigma}_{ij} = D_{ijkl}\varepsilon_{kl}(\boldsymbol{u}(t)) - \alpha\delta_{ij}p + \int_0^t \dot{\varphi}(t-s) D_{ijkl}\varepsilon_{kl}(\boldsymbol{u}(s))\, ds \tag{3}$$

for a constant $\alpha = \beta + \phi$.

Again from [25] we have for the pressure equation that

$$\nabla \cdot K\nabla p = (\phi\gamma + \zeta)\dot{p} + \alpha\delta_{ij}\dot{\varepsilon}_{ij} + \zeta \int_0^t \dot{\psi}(t-s)\dot{p}(s)\, ds \tag{4}$$

where $\gamma > 0$ denotes the fluid's compressibility and ζ the magnitude of the skeleton's viscoelastic compressibility. We assume a compressible porous medium so that $\zeta > 0$. It is, perhaps, helpful to remark that we are using slightly different notation to that introduced in [25]: in particular, ζ and η (see later) here correspond to $\hat{\mu}$ and $\tilde{\mu}$ there.

Integrating by parts, recalling that $p(0) = 0$, and (to match with the material in the Wheeler *et al.* papers cited earlier) setting $M = (\phi\gamma + \zeta)^{-1}$ we arrive at,

$$\nabla \cdot K\nabla p = \frac{1}{M}\dot{p} + \alpha\nabla \cdot \dot{\boldsymbol{u}} + \zeta\dot{\psi}(0)p(t) + \zeta p^*(t) \tag{5}$$

where the *internal pressure variable* is defined by

$$p^*(t) := \int_0^t \ddot{\psi}(t-s)p(s)\, ds = -\int_0^t \frac{\varphi_0\varphi_1}{\tau^2} e^{-\varphi_0(t-s)/\tau} p(s)\, ds \tag{6}$$

and, setting $\varphi_2 := \varphi_0\varphi_1/\tau \geqslant 0$ for convenience, satisfies

$$\tau\dot{p}^* + \varphi_0 p^* = -\varphi_2 p \qquad \text{subject to} \qquad p^*(0) = 0.$$

With these preliminaries complete we now move on to a formal statement of the problem that we want to consider.

Let $\Omega \subset \mathbb{R}^d$ be a bounded domain with polygonal/polyhedral boundary and let $I = (0, T]$ denote the time interval in which the solution is sought. With this viscoelastic modification we formulate the equations of initially quiescent quasistatic poroviscoelasticity, based

on the study in [25] and as an extension of the poroelasticity equations in [32], as,

$$\begin{aligned}
\frac{\partial}{\partial t}\left(\frac{1}{M}p + \alpha\nabla\cdot\boldsymbol{u}\right) + \nabla\cdot\boldsymbol{z} + \eta p &= q - \zeta p^*, &(7)\\
\boldsymbol{z} &= -K\nabla p, &(8)\\
-\nabla\cdot\tilde{\underline{\boldsymbol{\sigma}}} = -\nabla\cdot\underline{\boldsymbol{D}}\underline{\boldsymbol{\varepsilon}}(\boldsymbol{u}) + \nabla\cdot\underline{\boldsymbol{\sigma}}^* + \alpha\nabla p &= \boldsymbol{f}, &(9)\\
\tau\dot{\underline{\boldsymbol{\sigma}}}^* + \underline{\boldsymbol{\sigma}}^* &= \varphi_1\underline{\boldsymbol{D}}\underline{\boldsymbol{\varepsilon}}(\boldsymbol{u}), &(10)\\
\tau\dot{p}^* + \varphi_0 p^* &= -\varphi_2 p &(11)
\end{aligned}$$

where $\eta = \zeta\varphi_1/\tau$ and with given loads q, $\boldsymbol{f}$, initial data

$$p = 0,\ \boldsymbol{z} = \boldsymbol{0},\ \boldsymbol{u} = \boldsymbol{0},\ p^*(0) = 0 \text{ and } \underline{\boldsymbol{\sigma}}^* = \underline{\boldsymbol{0}}$$

in Ω at $t = 0$, and boundary data (with $\hat{\boldsymbol{n}}$ the unit outward normal to the boundary $\partial\Omega$),

$$\begin{aligned}
\boldsymbol{z}\cdot\hat{\boldsymbol{n}} &= \boldsymbol{z}^\flat\cdot\hat{\boldsymbol{n}} \quad \text{on } \Gamma_z, & p &= p^\flat \quad \text{on } \Gamma_p,\\
\boldsymbol{u} &= \boldsymbol{u}^\flat \quad \text{on } \Gamma_D, & \tilde{\sigma}_{ij}\hat{n}_j &= g_i \quad \text{on } \Gamma_N
\end{aligned}$$

where $\Gamma_N \cup \Gamma_D = \partial\Omega$ with $|\Gamma_D| > 0$ and $\Gamma_N \cap \Gamma_D = \varnothing$, and where $\Gamma_p \cup \Gamma_z = \partial\Omega$ with $\Gamma_p \cap \Gamma_z = \varnothing$. In this system we assume that φ_0, M, ζ, α, K and τ are positive constants, with φ_1 non-negative, and we are assuming quasistatic conditions (as in [18]) by neglecting the inertia term $\varrho\ddot{\boldsymbol{u}}$ in (9).

Our notation is standard and is introduced as we go along. We just note here that $\|\cdot\|_m := \|\cdot\|_{H^m(\Omega)}$ with no distinction being made for scalar-, vector- and tensor-valued functions, and we recall Young's inequality: $2ab \leqslant \epsilon a^2 + \epsilon^{-1}b^2$ for all $a, b \in \mathbb{R}$ and for all $\epsilon > 0$. Also because we are interested for the moment only in the model problem we will often assume that

$$\boldsymbol{z}^\flat = \boldsymbol{0}, \quad \boldsymbol{u}^\flat = \boldsymbol{0} \quad \text{and} \quad p^\flat = 0. \tag{12}$$

in order to simplify some of the arguments.

2 Weak formulation

Set $\boldsymbol{L}_2(\Omega) = L_2(\Omega)^d$, $\boldsymbol{H}^1(\Omega) = H^1(\Omega)^d$ and so on and define the linear and affine spaces,

$$\begin{aligned}
V_{\boldsymbol{g}} &= \left\{\boldsymbol{v} \in \boldsymbol{H}^1(\Omega)\colon \boldsymbol{v}|_{\Gamma_D} = \boldsymbol{g}\right\} \text{ with } V := V_{\boldsymbol{0}},\\
\boldsymbol{H}(\mathrm{div};\Omega) &= \left\{\boldsymbol{v} \in \boldsymbol{L}_2(\Omega)\colon \nabla\cdot\boldsymbol{v} \in L_2(\Omega)\right\},\\
\boldsymbol{H}_{\boldsymbol{g}}(\mathrm{div};\Omega) &= \left\{\boldsymbol{v} \in \boldsymbol{H}(\mathrm{div};\Omega)\colon \boldsymbol{v}\cdot\hat{\boldsymbol{n}} = \boldsymbol{g}\cdot\hat{\boldsymbol{n}} \text{ on } \Gamma_z\right\}.
\end{aligned}$$

Recall also that with the graph norm, $\|\boldsymbol{w}\|_{\boldsymbol{H}(\mathrm{div};\Omega)} := (\|\boldsymbol{w}\|_0^2 + \|\nabla\cdot\boldsymbol{w}\|_0^2)^{1/2}$ induced by the obvious inner product, $\boldsymbol{H}(\mathrm{div};\Omega)$ is a Hilbert space.

Recalling Green's formula,

$$\int_\Omega w_{,j}v\,d\Omega = -\int_\Omega wv_{,j}\,d\Omega + \oint_{\partial\Omega} wv\hat{n}_j\,d\Gamma,$$

and applying it to (9) we obtain first that for $\boldsymbol{v} \in V$,

$$-\int_\Omega \boldsymbol{v}\cdot(\nabla\cdot\tilde{\underline{\boldsymbol{\sigma}}})\,d\Omega = \int_\Omega \tilde{\sigma}_{ij}\varepsilon_{ij}(\boldsymbol{v})\,d\Omega - \oint_{\Gamma_N} g_i v_i\,d\Gamma,$$

and for the pressure term note that $\delta_{ij}\varepsilon_{ij}(\boldsymbol{v}) = \nabla\cdot\boldsymbol{v}$. Second, for $\boldsymbol{\psi}\in\boldsymbol{H}_0(\mathrm{div};\Omega)$,

$$\int_\Omega \boldsymbol{\psi}\cdot\nabla p\,d\Omega = -\int_\Omega \psi_{j,j}p\,d\Omega + \oint_{\partial\Omega} p\psi_j\hat{n}_j\,d\Gamma.$$

Hence,

$$\int_\Omega \boldsymbol{\psi}\cdot\nabla p\,d\Omega = -\int_\Omega p\nabla\cdot\boldsymbol{\psi}\,d\Omega + \oint_{\Gamma_p} p^\flat\boldsymbol{\psi}\cdot\hat{\boldsymbol{n}}\,d\Gamma.$$

and we are now led naturally to the weak problem in the following form:
find $(p,\boldsymbol{z},\boldsymbol{u},\underline{\boldsymbol{\sigma}}^*,p^*)\colon I\to L_2(\Omega)\times\boldsymbol{H}_{\boldsymbol{z}^\flat}(\mathrm{div};\Omega)\times V_{\boldsymbol{u}^\flat}\times\underline{\boldsymbol{L}}_2(\Omega)\times L_2(\Omega)$ such that,

$$(\tfrac{1}{M}\dot{p},\phi)+(\alpha\nabla\cdot\dot{\boldsymbol{u}},\phi)+(\nabla\cdot\boldsymbol{z},\phi)+(\eta p,\phi)+(\zeta p^*,\phi)=(q,\phi), \tag{13}$$

$$(p,\nabla\cdot\boldsymbol{\psi})-(K^{-1}\boldsymbol{z},\boldsymbol{\psi})=(p^\flat,\boldsymbol{\psi}\cdot\hat{\boldsymbol{n}})_{\Gamma_p}, \tag{14}$$

$$a(\boldsymbol{u},\boldsymbol{\chi})-(\underline{\boldsymbol{\sigma}}^*,\underline{\boldsymbol{\varepsilon}}(\boldsymbol{\chi}))-(\alpha p,\nabla\cdot\boldsymbol{\chi})=\langle L,\boldsymbol{\chi}\rangle, \tag{15}$$

$$(\tau\dot{\underline{\boldsymbol{\sigma}}}^*,\underline{\boldsymbol{\theta}})+(\underline{\boldsymbol{\sigma}}^*,\underline{\boldsymbol{\theta}})-(\varphi_1\underline{\boldsymbol{D}}\underline{\boldsymbol{\varepsilon}}(\boldsymbol{u}),\underline{\boldsymbol{\theta}})=0, \tag{16}$$

$$(\tau\dot{p}^*,\varpi)+(\varphi_0 p^*,\varpi)+(\varphi_2 p,\varpi)=0, \tag{17}$$

$$\forall\phi\in L_2(\Omega),\ \forall\boldsymbol{\psi}\in\boldsymbol{H}_0(\mathrm{div};\Omega),\ \forall\boldsymbol{\chi}\in V,\ \forall\underline{\boldsymbol{\theta}}\in\underline{\boldsymbol{L}}_2(\Omega),\ \forall\varpi\in L_2(\Omega)$$

and where $\langle L,\boldsymbol{\chi}\rangle := (\boldsymbol{f},\boldsymbol{\chi})+(\boldsymbol{g},\boldsymbol{\chi})_{\Gamma_N}$ and $a(\boldsymbol{u},\boldsymbol{\chi}) := (\underline{\boldsymbol{D}}\underline{\boldsymbol{\varepsilon}}(\boldsymbol{u}),\underline{\boldsymbol{\varepsilon}}(\boldsymbol{\chi}))$. For use below (as is standard for elasticity problems) we define an energy norm via $\|\cdot\|_V := a(\cdot,\cdot)^{1/2}$. Note that we require $\boldsymbol{f}=\boldsymbol{g}=\boldsymbol{0}$ at $t=0$.

Our first result is a basic stability estimate. As is usual for linear problems this will inform the structure of the discrete stability estimate, Prop. 3.2, as well as the main error bound, Lemma 4.1.

Proposition 2.1 (stability) *With* (12)*,*

$$\begin{aligned}&\|\boldsymbol{u}(t)\|_V^2+\|M^{-1/2}p(t)\|_0^2+\|\underline{\boldsymbol{\sigma}}^*(t)\|_0^2+\|p^*(t)\|_0^2+\eta\|p\|^2_{L_2(0,t;L_2(\Omega))}\\ &\quad+\|\underline{\boldsymbol{\sigma}}^*\|^2_{L_2(0,t;\underline{\boldsymbol{L}}_2(\Omega))}+\|p^*\|^2_{L_2(0,t;L_2(\Omega))}+\|\tau^{1/2}\dot{\underline{\boldsymbol{\sigma}}}^*\|^2_{L_2(0,t;\underline{\boldsymbol{L}}_2(\Omega))}+\|\dot{p}^*\|^2_{L_2(0,t;L_2(\Omega))}\\ &\quad+\|K^{-1/2}\boldsymbol{z}\|^2_{L_2(0,t;\boldsymbol{L}_2(\Omega))}\leqslant C\Big(\|M^{1/2}q\|^2_{L_2(0,t;L_2(\Omega))}+\|\boldsymbol{f}\|^2_{H^1(0,t;V')}+\|\boldsymbol{g}\|^2_{H^1(0,t;\boldsymbol{L}_2(\Gamma_N))}\Big)\end{aligned}$$

for all $t\in I$*.*

Proof. Choose $\boldsymbol{\chi}=\dot{\boldsymbol{u}}$, $\phi=p$ and $\boldsymbol{\psi}=-\boldsymbol{z}$ in (13), (14) and (15), and add to get,

$$\begin{aligned}&a(\boldsymbol{u},\dot{\boldsymbol{u}})-(\alpha p,\nabla\cdot\dot{\boldsymbol{u}})+(M^{-1}\dot{p},p)+(\alpha\nabla\cdot\dot{\boldsymbol{u}},p)\\ &\qquad+(\nabla\cdot\boldsymbol{z},p)+\eta(p,p)+\zeta(p,p^*)+(K^{-1}\boldsymbol{z},\boldsymbol{z})-(p,\nabla\cdot\boldsymbol{z})\\ &\qquad\qquad=(\boldsymbol{f},\dot{\boldsymbol{u}})+(\boldsymbol{g},\dot{\boldsymbol{u}})_{\Gamma_N}+(\underline{\boldsymbol{\sigma}}^*,\underline{\boldsymbol{\varepsilon}}(\dot{\boldsymbol{u}}))+(q,p).\end{aligned}$$

Hence, on noting the double cancellation, we get,

$$\begin{aligned}\frac{d}{dt}\Big(\|\boldsymbol{u}\|_V^2+\|M^{-1/2}p\|_0^2\Big)+2\|K^{-1/2}\boldsymbol{z}\|_0^2+2\eta\|p\|_0^2&=2(\boldsymbol{f},\dot{\boldsymbol{u}})\\ &\quad+2(\boldsymbol{g},\dot{\boldsymbol{u}})_{\Gamma_N}+2(\underline{\boldsymbol{\sigma}}^*,\underline{\boldsymbol{\varepsilon}}(\dot{\boldsymbol{u}}))+2(q,p)-2\zeta(p,p^*).\end{aligned}$$

Now we choose $\underline{\boldsymbol{\theta}} = 2\underline{\boldsymbol{\sigma}}^*$ in (16) and arrive at

$$\frac{d}{dt}\|\tau^{1/2}\underline{\boldsymbol{\sigma}}^*\|_0^2 + 2\|\underline{\boldsymbol{\sigma}}^*\|_0^2 = 2(\varphi_1 \underline{\boldsymbol{D}}\underline{\boldsymbol{\varepsilon}}(\boldsymbol{u}), \underline{\boldsymbol{\sigma}}^*),$$

and then, for some constant $\vartheta \in \mathbb{R}_+$, we may also choose $\underline{\boldsymbol{\theta}} = 2\vartheta\dot{\underline{\boldsymbol{\sigma}}}^*$ in (16) to get,

$$\vartheta\frac{d}{dt}\|\underline{\boldsymbol{\sigma}}^*\|_0^2 + 2\vartheta\|\tau^{1/2}\dot{\underline{\boldsymbol{\sigma}}}^*\|_0^2 = 2\vartheta(\varphi_1 \underline{\boldsymbol{D}}\underline{\boldsymbol{\varepsilon}}(\boldsymbol{u}), \dot{\underline{\boldsymbol{\sigma}}}^*).$$

Similarly, in (17) we choose first $\varpi = 2p^*$ to get

$$\frac{d}{dt}\|\tau^{1/2}p^*\|_0^2 + 2\varphi_0\|p^*\|_0^2 = -2\varphi_2(p, p^*),$$

and then choose $\varpi = 2\dot{p}^*$ to get

$$\frac{d}{dt}\|\varphi_0^{1/2}p^*\|_0^2 + 2\tau\|\dot{p}^*\|_0^2 = -2\varphi_2(p, \dot{p}^*).$$

Incorporating both of these then yields,

$$\begin{aligned}
&\frac{d}{dt}\Big(\|\boldsymbol{u}\|_V^2 + \|M^{-1/2}p\|_0^2 + \vartheta\|\underline{\boldsymbol{\sigma}}^*\|_0^2 + \|\tau^{1/2}\underline{\boldsymbol{\sigma}}^*\|_0^2 + \|\tau^{1/2}p^*\|_0^2 + \|\varphi_0^{1/2}p^*\|_0^2\Big) \\
&\quad + 2\|K^{-1/2}\boldsymbol{z}\|_0^2 + 2\vartheta\|\tau^{1/2}\dot{\underline{\boldsymbol{\sigma}}}^*\|_0^2 + 2\|\underline{\boldsymbol{\sigma}}^*\|_0^2 + 2\eta\|p\|_0^2 + 2\varphi_0\|p^*\|_0^2 + 2\tau\|\dot{p}^*\|_0^2 = 2(\boldsymbol{f}, \dot{\boldsymbol{u}}) \\
&\qquad + 2(\boldsymbol{g}, \dot{\boldsymbol{u}})_{\Gamma_N} + 2(\underline{\boldsymbol{\sigma}}^*, \underline{\boldsymbol{\varepsilon}}(\dot{\boldsymbol{u}})) + 2(q, p) - 2\zeta(p, p^*) - 2\varphi_2(p, p^*) - 2\varphi_2(p, \dot{p}^*) \\
&\qquad\qquad + 2\vartheta(\varphi_1 \underline{\boldsymbol{D}}\underline{\boldsymbol{\varepsilon}}(\boldsymbol{u}), \dot{\underline{\boldsymbol{\sigma}}}^*) + 2(\varphi_1 \underline{\boldsymbol{D}}\underline{\boldsymbol{\varepsilon}}(\boldsymbol{u}), \underline{\boldsymbol{\sigma}}^*).
\end{aligned}$$

Integrating over $(0, t)$ and then integrating by parts in the first three terms on the right now gives,

$$\begin{aligned}
&2\int_0^t \|K^{-1/2}\boldsymbol{z}(s)\|_0^2 + \vartheta\|\tau^{1/2}\dot{\underline{\boldsymbol{\sigma}}}^*(s)\|_0^2 + \|\underline{\boldsymbol{\sigma}}^*(s)\|_0^2 + \eta\|p(s)\|_0^2 + \varphi_0\|p^*(s)\|_0^2 + \tau\|\dot{p}^*(s)\|_0^2\, ds \\
&+ \|\boldsymbol{u}(t)\|_V^2 + \|M^{-1/2}p(t)\|_0^2 + \vartheta\|\underline{\boldsymbol{\sigma}}^*(t)\|_0^2 + \|\tau^{1/2}\underline{\boldsymbol{\sigma}}^*(t)\|_0^2 + \|\tau^{1/2}p^*(t)\|_0^2 + \|\varphi_0^{1/2}p^*(t)\|_0^2 \\
&\qquad = 2\int_0^t (q(s), p(s)) - (\zeta + \varphi_2)(p(s), p^*(s)) - \varphi_2(p(s), \dot{p}^*(s))\, ds \\
&\qquad\quad + 2\int_0^t \vartheta(\varphi_1 \underline{\boldsymbol{D}}\underline{\boldsymbol{\varepsilon}}(\boldsymbol{u}(s)), \dot{\underline{\boldsymbol{\sigma}}}^*(s)) + (\varphi_1 \underline{\boldsymbol{D}}\underline{\boldsymbol{\varepsilon}}(\boldsymbol{u}(s)), \underline{\boldsymbol{\sigma}}^*(s))\, ds \\
&\qquad\qquad + 2(\boldsymbol{f}(t), \boldsymbol{u}(t)) - 2(\boldsymbol{f}(0), \breve{\boldsymbol{u}}) + 2(\boldsymbol{g}(t), \boldsymbol{u}(t))_{\Gamma_N} \\
&\qquad\quad - 2(\boldsymbol{g}(0), \breve{\boldsymbol{u}})_{\Gamma_N} + 2(\underline{\boldsymbol{\sigma}}^*(t), \underline{\boldsymbol{\varepsilon}}(\boldsymbol{u}(t)) - 2\int_0^t (\dot{\boldsymbol{f}}(s), \boldsymbol{u}(s))\, ds \\
&\qquad\qquad\qquad - 2\int_0^t (\dot{\boldsymbol{g}}(s), \boldsymbol{u}(s))_{\Gamma_N} + (\dot{\underline{\boldsymbol{\sigma}}}^*(s), \underline{\boldsymbol{\varepsilon}}(\boldsymbol{u}(s)))\, ds.
\end{aligned}$$

To finish the proof we will handle the first term on the right with Gronwall's inequality, the second and third (resp. fourth and fifth) terms with a Gronwall estimate for terms in p (resp. $\boldsymbol{u}$) and a kickback for the p^* (resp. $\underline{\boldsymbol{\sigma}}^*$) terms. For terms six to nine we recall that the initial data are zero and then can kick back $\boldsymbol{u}$ while the entire term ten can be kicked-back with a suitable choice for ϑ. Terms eleven and twelve can be handled with

Gronwall's inequality again, as can term thirteen with a kickback on the internal variable. Thus, by Young's inequality, we have the following estimates,

$$2\int_0^t (q(s),p(s))\,ds \leqslant \int_0^t \|M^{1/2}q(s)\|_0^2 + \|M^{-1/2}p(s)\|_0^2\,ds,$$

$$2\int_0^t (\zeta+\varphi_2)(p(s),p^*(s))\,ds + 2\int_0^t \varphi_2(p(s),\dot{p}^*(s))\,ds \leqslant \int_0^t \varphi_0\|p^*(s)\|_0^2\,ds + \int_0^t \tau\|\dot{p}^*(s)\|_0^2\,ds + \left(\frac{(\zeta+\varphi_2)^2M}{\varphi_0} + \frac{\varphi_2^2M}{\tau}\right)\int_0^t \|M^{-1/2}p(s)\|_0^2\,ds,$$

$$2\vartheta\int_0^t (\varphi_1 \underline{\boldsymbol{D}}\underline{\boldsymbol{\varepsilon}}(\boldsymbol{u}(s)),\dot{\underline{\boldsymbol{\sigma}}}^*(s))\,ds \leqslant \epsilon_4\vartheta\int_0^t \|\tau^{1/2}\dot{\underline{\boldsymbol{\sigma}}}^*(s)\|_0^2\,ds + \frac{\varphi_1^2\vartheta\|\underline{\boldsymbol{D}}\|_{\underline{\boldsymbol{L}}_\infty(\Omega)}}{\tau\epsilon_4}\int_0^t \|\boldsymbol{u}(s)\|_V^2\,ds,$$

$$2\int_0^t (\varphi_1\boldsymbol{D}\boldsymbol{\varepsilon}(\boldsymbol{u}(s)),\boldsymbol{\sigma}^*(s))\,ds \leqslant \int_0^t \|\boldsymbol{\sigma}^*(s)\|_0^2\,ds + \varphi_1^2\|\boldsymbol{D}\|_{\underline{\boldsymbol{L}}_\infty(\Omega)}\int_0^t \|\boldsymbol{u}(s)\|_V^2\,ds,$$

$$2(\boldsymbol{f}(t),\boldsymbol{u}(t)) - 2(\boldsymbol{f}(0),\breve{\boldsymbol{u}}) \leqslant \epsilon_6\|\boldsymbol{u}(t)\|_V^2 + \frac{1}{\epsilon_6}\|\boldsymbol{f}\|^2_{L_\infty(0,t;V')},$$

$$2(\boldsymbol{g}(t),\boldsymbol{u}(t))_{\Gamma_N} - 2(\boldsymbol{g}(0),\breve{\boldsymbol{u}})_{\Gamma_N} \leqslant \epsilon_8\|\boldsymbol{u}(t)\|_V^2 + \frac{C}{\epsilon_8}\|\boldsymbol{g}\|^2_{L_\infty(0,t;\boldsymbol{L}_2(\Gamma_N))},$$

$$2(\underline{\boldsymbol{\sigma}}^*(t),\underline{\boldsymbol{\varepsilon}}(\boldsymbol{u})) \leqslant \frac{\|\underline{\boldsymbol{D}}^{-1}\|_{\underline{\boldsymbol{L}}_\infty(\Omega)}}{\epsilon_{10}}\|\underline{\boldsymbol{\sigma}}^*(t)\|_0^2 + \epsilon_{10}\|\boldsymbol{u}(t)\|_V^2,$$

$$2\int_0^t (\dot{\boldsymbol{f}}(s),\boldsymbol{u}(s))\,ds + 2\int_0^t (\dot{\boldsymbol{g}}(s),\boldsymbol{u}(s))_{\Gamma_N}\,ds \leqslant \|\dot{\boldsymbol{f}}\|^2_{L_2(0,t;V')} + C\|\dot{\boldsymbol{g}}\|^2_{L_2(0,t;\boldsymbol{L}_2(\Gamma_N)} + 2\int_0^t \|\boldsymbol{u}(s)\|_V^2\,ds,$$

$$2\int_0^t (\dot{\underline{\boldsymbol{\sigma}}}^*(s),\underline{\boldsymbol{\varepsilon}}(\boldsymbol{u}(s))\,ds \leqslant \vartheta\epsilon_{13}\int_0^t \|\tau^{1/2}\dot{\underline{\boldsymbol{\sigma}}}^*(s)\|_0^2\,ds + \frac{\|\tau^{-1}\underline{\boldsymbol{D}}^{-1}\|_{\underline{\boldsymbol{L}}_\infty(\Omega)}}{\vartheta\epsilon_{13}}\int_0^t \|\boldsymbol{u}(s)\|_V^2\,ds.$$

Hence,

$$\begin{aligned}
&(1-\epsilon_6-\epsilon_8-\epsilon_{10})\|\boldsymbol{u}(t)\|_V^2 + \|M^{-1/2}p(t)\|_0^2 + \left(\vartheta - \frac{\|\underline{\boldsymbol{D}}^{-1}\|_{\underline{\boldsymbol{L}}_\infty(\Omega)}}{\epsilon_{10}}\right)\|\underline{\boldsymbol{\sigma}}^*(t)\|_0^2 \\
&+ \|\tau^{1/2}\underline{\boldsymbol{\sigma}}^*(t)\|_0^2 + \|\tau^{1/2}p^*(t)\|_0^2 + \|\varphi_0^{1/2}p^*(t)\|_0^2 + 2\int_0^t \|K^{-1/2}\boldsymbol{z}(s)\|_0^2\,ds + \int_0^t \|\underline{\boldsymbol{\sigma}}^*(s)\|_0^2\,ds \\
&+ \int_0^t \eta\|p(s)\|_0^2 + \varphi_0\|p^*(s)\|_0^2 + \tau\|\dot{p}^*(s)\|_0^2\,ds + (2\vartheta - \epsilon_4\vartheta - \epsilon_{13}\vartheta)\int_0^t \|\tau^{1/2}\dot{\underline{\boldsymbol{\sigma}}}^*(s)\|_0^2\,ds \\
&\leqslant \frac{1}{\epsilon_6}\|\boldsymbol{f}\|^2_{L_\infty(0,t;V')} + \|\dot{\boldsymbol{f}}\|^2_{L_2(0,t;V')} + \frac{C}{\epsilon_8}\|\boldsymbol{g}\|^2_{L_\infty(0,t;\boldsymbol{L}_2(\Gamma_N))} + C\|\dot{\boldsymbol{g}}\|^2_{L_2(0,t;\boldsymbol{L}_2(\Gamma_N))} \\
&+ \|M^{1/2}q\|^2_{L_2(0,t;L_2(\Omega))} + \left(1 + \frac{(\zeta+\varphi_2)^2M}{\varphi_0} + \frac{\varphi_2^2M}{\tau}\right)\int_0^t \|M^{-1/2}p(s)\|_0^2\,ds \\
&+ \left(2 + \frac{\varphi_1^2\vartheta\|\underline{\boldsymbol{D}}\|_{\underline{\boldsymbol{L}}_\infty(\Omega)}}{\tau\epsilon_4} + \frac{\|\tau^{-1}\underline{\boldsymbol{D}}^{-1}\|_{\underline{\boldsymbol{L}}_\infty(\Omega)}}{\vartheta\epsilon_{13}} + \varphi_1^2\|\underline{\boldsymbol{D}}\|_{\underline{\boldsymbol{L}}_\infty(\Omega)}\right)\int_0^t \|\boldsymbol{u}(s)\|_V^2\,ds.
\end{aligned}$$

We can now choose $\epsilon_6 = \epsilon_8 = \epsilon_{10} = 1/6$ and $\epsilon_4 = \epsilon_{13} = 1/2$, set $\vartheta = 1/2 + 6\|\underline{\boldsymbol{D}}^{-1}\|_{\underline{\boldsymbol{L}}_\infty(\Omega)}$, and then complete the proof by using the Sobolev estimate $\|\cdot\|_{L_\infty(0,t;\cdot)} \leqslant C\|\cdot\|_{H^1(0,t;\cdot)}$ and then applying Gronwall's inequality. ∎

Corollary 2.2 *Under the same hypotheses as above we also have that* $\|\boldsymbol{u}\|_{L_2(0,t;V)}$ *is bounded by data.*

Proof. $\|\boldsymbol{u}(t)\|_V^2 \leqslant C(\|\tau^{1/2}\dot{\underline{\boldsymbol{\sigma}}}^*(t)\|_0^2 + \|\underline{\boldsymbol{\sigma}}^*(t)\|_0^2)$ follows from (16) and the stability estimate given above provides the desired bound. ∎

3 Numerical scheme

For the time discretisation we choose an $N \in \mathbb{N}$ and set $t_i = ik$ where $k = T/N$ is the time step. We write $w(t_i) = w_i$ and so on, define ∂_t by the differencing rule $\partial_t w_i := (w_i - w_{i-1})/k$ and for later use recall the identity $2k(\partial_t w_i, w_i) = k\partial_t\|w_i\|_0^2 + k^2\|\partial_t w_i\|_0^2$. The second term on the right will play a useful role in establishing stability of the discrete problem—see later in (23).

Relative to a given triangluation, T^h, let: $W^h \subset L_2(\Omega)$ be the space of piecewise constants; $V^h \subset V$ be the standard piecewise linear conforming finite element space; and $\mathrm{RT}^h_{\boldsymbol{z}^\flat} \subset \boldsymbol{H}_{\boldsymbol{z}^\flat}(\mathrm{div};\Omega)$ be the Raviart-Thomas lowest order space with $\mathrm{RT}^h := \mathrm{RT}^h_{\boldsymbol{0}}$. With all initial data set to zero, our backward-Euler mixed and Galerkin finite element method for the weak problem (13)—(17) is then: for $i = 1, 2, \ldots, N$, find $(p_i^h, \boldsymbol{z}_i^h, \boldsymbol{u}_i^h, \underline{\boldsymbol{\sigma}}_i^{*h}, p_i^{*h}) \in W^h \times \mathrm{RT}^h \times V^h_{\boldsymbol{u}^\flat} \times \underline{\boldsymbol{W}}^h \times W^h$ such that,

$$(\tfrac{1}{M}\partial_t p_i^h + \nabla\cdot\boldsymbol{z}_i^h, \phi) + (\alpha\nabla\cdot\partial_t\boldsymbol{u}_i^h, \phi) + (\zeta p_i^{*h} + \eta p_i^h, \phi) = (q_i, \phi), \tag{18}$$

$$(p_i^h, \nabla\cdot\boldsymbol{\psi}) - (K^{-1}\boldsymbol{z}_i^h, \boldsymbol{\psi}) = (p_i^\flat, \boldsymbol{\psi}\cdot\hat{\boldsymbol{n}})_{\Gamma_p}, \tag{19}$$

$$a(\boldsymbol{u}_i^h, \boldsymbol{\chi}) - (\underline{\boldsymbol{\sigma}}_i^{*h}, \underline{\boldsymbol{\varepsilon}}(\boldsymbol{\chi})) - (\alpha p_i^h, \nabla\cdot\boldsymbol{\chi}) = \langle L_i, \boldsymbol{\chi}\rangle, \tag{20}$$

$$(\tau\partial_t\underline{\boldsymbol{\sigma}}_i^{*h}, \underline{\boldsymbol{\theta}}) + (\underline{\boldsymbol{\sigma}}_i^{*h}, \underline{\boldsymbol{\theta}}) = (\varphi_1\underline{\boldsymbol{D}}\underline{\boldsymbol{\varepsilon}}(\beth_m\boldsymbol{u}_i^h), \underline{\boldsymbol{\theta}}), \tag{21}$$

$$(\tau\partial_t p_i^{*h}, \varpi) + (\varphi_0 p_i^{*h}, \varpi) = -(\varphi_2\beth_m p_i^h, \varpi), \tag{22}$$

$$\forall\phi \in W^h,\ \forall\boldsymbol{\psi} \in \mathrm{RT}^h,\ \forall\boldsymbol{\chi} \in V^h,\ \forall\underline{\boldsymbol{\theta}} \in \underline{\boldsymbol{W}}^h,\ \forall\varpi \in W^h,$$

and where $\langle L_i, \boldsymbol{\chi}\rangle := (\boldsymbol{f}(t_i), \boldsymbol{\chi}) + (\boldsymbol{g}(t_i), \boldsymbol{\chi})_{\Gamma_N}$. Also, in (21) and (22), we have introduced a shifting, or 'lagging', operator defined through $\beth_m v_i := v_{i-m}$, but we will only be concerned with the cases $m = 0$ and $m = 1$. The former is in some way the 'natural' choice for an implicit Euler discretisation while the latter represents a 'lagging' (in the sense of Lowrie, [14]). We shall see below in Prop. 3.2 that the lagged scheme is stable for all time step sizes while the natural scheme appears to be only conditionally stable.

In the case of $\beth_1$ it is clear that the viscoelastic stress and pressure calculations can be performed independently of the displacement, pressure and flux calculations due to the lagging. Also, for $\beth_0$ we notice that this calculation can still be performed outside of the displacement calculation since,

$$((\tau + k)\underline{\boldsymbol{\sigma}}_i^{*h}, \underline{\boldsymbol{\theta}}) = (k\varphi_1\underline{\boldsymbol{D}}\underline{\boldsymbol{\varepsilon}}(\boldsymbol{u}_i^h), \underline{\boldsymbol{\theta}}) + (\tau\underline{\boldsymbol{\sigma}}_{i-1}^{*h}, \underline{\boldsymbol{\theta}}),$$

(for all $\underline{\boldsymbol{\theta}} \in \underline{\boldsymbol{W}}^h$) yields $\underline{\boldsymbol{\sigma}}_i^{*h}$ once $\boldsymbol{u}_i^h$ is known. Taking $\underline{\boldsymbol{\theta}} = (\tau + k)^{-1}\underline{\boldsymbol{\varepsilon}}(\boldsymbol{\chi}) \in \underline{\boldsymbol{W}}^h$ and substituting into the displacement equation then produces,

$$\begin{aligned} a\left(\tfrac{\tau+\varphi_0 k}{\tau+k}\boldsymbol{u}_i^h, \boldsymbol{\chi}\right) - (\alpha p_i^h, \nabla\cdot\boldsymbol{\chi}) &= (\boldsymbol{f}_i, \boldsymbol{\chi}) + (\boldsymbol{g}_i, \boldsymbol{\chi})_{\Gamma_N} \\ &+ \left(\tfrac{\tau}{\tau+k}\underline{\boldsymbol{\sigma}}_{i-1}^{*h}, \underline{\boldsymbol{\varepsilon}}(\boldsymbol{\chi})\right) \qquad \forall \boldsymbol{\chi} \in V^h, \end{aligned}$$

since $1 - \varphi_1 k/(\tau + k) = (\tau + \varphi_0 k)/(\tau + k)$ according to our earlier definition of the stress relaxation function. Hence, at any given time level we can solve for displacement, pressure and flux using the previous viscous stress, and then update the viscous stress prior to advancing to the next time level.

In a similar way, (22) can be written in the case of $\dashv_0$ as

$$((\tau + \varphi_0 k)p_i^{*h}, \varpi) = (\tau p_{i-1}^{*h} - k\varphi_2 p_i^h, \varpi)$$

and by choosing $\varpi = \zeta\phi/(\tau + \varphi_0 k)$ and substituting into the pressure equation, (18), we arrive at,

$$(\tfrac{1}{M}\partial_t p_i^h + \nabla\cdot\boldsymbol{z}_i^h, \phi) + (\alpha\nabla\cdot\partial_t\boldsymbol{u}_i^h, \phi) + \left(\left(\eta - \tfrac{\zeta k\varphi_2}{\tau+\varphi_0 k}\right)p_i^h, \phi\right) = (q_i, \phi) - \left(\tfrac{\zeta\tau}{\tau+\varphi_0 k}p_{i-1}^{*h}, \phi\right).$$

Recalling that $\eta = \zeta\varphi_1/\tau$ and $\varphi_2 = \varphi_0\varphi_1/\tau$ we easily obtain the simplification $\eta - \zeta k\varphi_2/(\tau + k\varphi_0) = \zeta\varphi_1/(\tau + k\varphi_0) \geqslant 0$ with equality only when $\varphi_1 = 0$ (since $\zeta > 0$). This re-formulation does not, therefore, affect the well-posedness of the problem.

Remark 3.1 *First, notice that we can get back to poroelasticity simply by taking $\varphi_0 = 1$ (so that $\varphi_1 = 0$). Conversely, any poroelasticity solver can be turned into a poroviscoelasticity solver by simply adding four functionalities.*

1. *The extra "reaction" term and viscous pressure load needs to be incorporated into the pressure equation,* (18).

2. *The extra viscous stress loading needs to be included in the right hand side of the displacement equation,* (20).

3. *For the $\dashv_0$ scheme the Lamé coefficients need to be replaced by modified vales according to the replacements*

$$\lambda \leftarrow \frac{\tau + \varphi_0 k}{\tau + k}\lambda \qquad \textit{and} \qquad \mu \leftarrow \frac{\tau + \varphi_0 k}{\tau + k}\mu.$$

   The lagged scheme does not need this modification.

4. *The viscous stress (resp. pressure) update arising from* (21) *(resp.* (22)*) needs to be coded. In the case considered here this is simply an $\underline{\boldsymbol{L}}_2(\Omega)$ (resp. $L_2(\Omega)$) projection on to tensor (resp. scalar) piecewise-constants.*

We now give a stability estimate for the discrete scheme. The assumption $\varphi_1 > 0$ (instead of $\varphi_1 \geqslant 0$) is made because (see Remark 3.1) with $\varphi_1 = 0$ we are back to the known case of poroelasticity.

Proposition 3.2 (discrete stability) *With* (12), $\varphi_1 > 0$ *and for small enough time step in the case of* $\beth_0$*, we have,*

$$
\begin{aligned}
k\sum_{i=1}^{j}\Big(\|K^{-1/2}\boldsymbol{z}_i^h\|_0^2 + \|\underline{\boldsymbol{\sigma}}_i^{*h}\|_0^2 + \|\tau^{1/2}\partial_t\underline{\boldsymbol{\sigma}}_i^{*h}\|_0^2 + \|p_i^h\|_0^2 + \|p_i^{*h}\|_0^2 + \|\partial_t p_i^{*h}\|_0^2\Big) \\
+ k^2\sum_{i=1}^{j}\Big(\|M^{-1/2}\partial_t p_i^h\|_0^2 + \|\partial_t p_i^{*h}\|_0^2 + \|\tau^{1/2}\partial_t\underline{\boldsymbol{\sigma}}_i^{*h}\|_0^2 + \|\partial_t\boldsymbol{u}_i^h\|_V^2\Big) \\
+ \|\boldsymbol{u}_j^h\|_V^2 + \|M^{-1/2}p_j^h\|_0^2 + \|\underline{\boldsymbol{\sigma}}_j^{*h}\|_0^2 + \|p_j^{*h}\|_0^2 \\
\leqslant C\Big(\|\boldsymbol{f}\|_{H^1(0,t_j;V')}^2 + \|\boldsymbol{g}\|_{H^1(0,t_j;\boldsymbol{L}_2(\Gamma_N))}^2 + \|M^{1/2}q\|_{L_\infty(0,t_j;L_2(\Omega))}^2\Big)
\end{aligned}
$$

for all $j \leqslant N$.

Proof. In (18), (19) and (20) we choose $\phi = p_i^h$, $\boldsymbol{\psi} = -\boldsymbol{z}_i^h$ and $\boldsymbol{\chi} = \partial_t\boldsymbol{u}_i^h$, add the resulting equations and multiply by $2k$ to get,

$$
\begin{aligned}
k\partial_t\|M^{-1/2}p_i^h\|_0^2 + k\partial_t\|\boldsymbol{u}_i^h\|_V^2 + 2k\|K^{-1/2}\boldsymbol{z}_i^h\|_0^2 + 2k\eta\|p_i^h\|_0^2 \\
+ k^2\|M^{-1/2}\partial_t p_i^h\|_0^2 + k^2\|\partial_t\boldsymbol{u}_i^h\|_V^2 = 2k(q_i, p_i^h) - 2k\zeta(p_i^h, p_i^{*h}) \\
+ 2k(\boldsymbol{f}_i, \partial_t\boldsymbol{u}_i^h) + 2k(\boldsymbol{g}_i, \partial_t\boldsymbol{u}_i^h)_{\Gamma_N} + 2k(\underline{\boldsymbol{\sigma}}_i^{*h}, \underline{\boldsymbol{\varepsilon}}(\partial_t\boldsymbol{u}_i^h)).
\end{aligned}
$$

Now in (21) choose $\underline{\boldsymbol{\theta}} = 2k\kappa\underline{\boldsymbol{\sigma}}_i^{*h}$ to get,

$$
\kappa k\partial_t\|\tau^{1/2}\underline{\boldsymbol{\sigma}}_i^{*h}\|_0^2 + 2k\kappa\|\underline{\boldsymbol{\sigma}}_i^{*h}\|_0^2 + \kappa k^2\|\tau^{1/2}\partial_t\underline{\boldsymbol{\sigma}}_i^{*h}\|_0^2 = 2k\kappa(\varphi_1\underline{\boldsymbol{D}}\underline{\boldsymbol{\varepsilon}}(\beth_m\boldsymbol{u}_i^h), \underline{\boldsymbol{\sigma}}_i^{*h}),
$$

and then choose $\underline{\boldsymbol{\theta}} = 2k\vartheta\partial_t\underline{\boldsymbol{\sigma}}_i^{*h}$ to get,

$$
\vartheta k\partial_t\|\underline{\boldsymbol{\sigma}}_i^{*h}\|_0^2 + 2\vartheta k\|\tau^{1/2}\partial_t\underline{\boldsymbol{\sigma}}_i^{*h}\|_0^2 + \vartheta k^2\|\partial_t\underline{\boldsymbol{\sigma}}_i^{*h}\|_0^2 = 2\vartheta k(\varphi_1\underline{\boldsymbol{D}}\underline{\boldsymbol{\varepsilon}}(\beth_m\boldsymbol{u}_i^h), \partial_t\underline{\boldsymbol{\sigma}}_i^{*h}).
$$

Here $\kappa, \vartheta \in \mathbb{R}_+$ are constants that will be specified later. Also, for two other positive constants, ρ and ϱ, we choose $\varpi = 2\rho k p_i^{*h}$ in (22) to get

$$
2k\rho\varphi_0\|p_i^{*h}\|_0^2 + \tau\rho k\partial_t\|p_i^{*h}\|_0^2 + \tau\rho k^2\|\partial_t p_i^{*h}\|_0^2 = -2k\rho\varphi_2(\beth_m p_i^h, p_i^{*h}),
$$

and then $\varpi = 2\varrho k\partial_t p_i^{*h}$ to get,

$$
2\varrho\tau k\|\partial_t p_i^{*h}\|_0^2 + \varrho k\varphi_0\partial_t\|p_i^{*h}\|_0^2 + \varrho\varphi_0 k^2\|\partial_t p_i^{*h}\|_0^2 = -2k\varrho\varphi_2(\beth_m p_i^h, \partial_t p_i^{*h}).
$$

Assembling these results into the main expression above then yields,

$$
\begin{aligned}
k\partial_t\Big(\|M^{-1/2}p_i^h\|_0^2 + \|\boldsymbol{u}_i^h\|_V^2 + \kappa\|\tau^{1/2}\underline{\boldsymbol{\sigma}}_i^{*h}\|_0^2 + \vartheta\|\underline{\boldsymbol{\sigma}}_i^{*h}\|_0^2 + (\varrho\varphi_0 + \rho\tau)\|p_i^{*h}\|_0^2\Big) \\
+ 2k\Big(\|K^{-1/2}\boldsymbol{z}_i^h\|_0^2 + \eta\|p_i^h\|_0^2 + \kappa\|\underline{\boldsymbol{\sigma}}_i^{*h}\|_0^2 + \vartheta\|\tau^{1/2}\partial_t\underline{\boldsymbol{\sigma}}_i^{*h}\|_0^2 + \varrho\tau\|\partial_t p_i^{*h}\|_0^2 + \rho\varphi_0\|p_i^{*h}\|_0^2\Big) \\
+ k^2\Big(\|M^{-1/2}\partial_t p_i^h\|_0^2 + \|\partial_t\boldsymbol{u}_i^h\|_V^2 + \kappa\|\tau^{1/2}\partial_t\underline{\boldsymbol{\sigma}}_i^{*h}\|_0^2 + \vartheta\|\partial_t\underline{\boldsymbol{\sigma}}_i^{*h}\|_0^2 + (\varrho\varphi_0 + \rho\tau)\|\partial_t p_i^{*h}\|_0^2\Big) \\
= 2k(q_i, p_i^h) - 2k\zeta(p_i^h, p_i^{*h}) + 2k(\boldsymbol{f}_i, \partial_t\boldsymbol{u}_i^h) + 2k(\boldsymbol{g}_i, \partial_t\boldsymbol{u}_i^h)_{\Gamma_N} + 2k(\underline{\boldsymbol{\sigma}}_i^{*h}, \underline{\boldsymbol{\varepsilon}}(\partial_t\boldsymbol{u}_i^h)) \\
+ 2k\kappa(\varphi_1\underline{\boldsymbol{D}}\underline{\boldsymbol{\varepsilon}}(\beth_m\boldsymbol{u}_i^h), \underline{\boldsymbol{\sigma}}_i^{*h}) + 2k\vartheta(\varphi_1\underline{\boldsymbol{D}}\underline{\boldsymbol{\varepsilon}}(\beth_m\boldsymbol{u}_i^h), \partial_t\underline{\boldsymbol{\sigma}}_i^{*h}) \\
- 2\varrho k\varphi_2(\beth_m p_i^h, \partial_t p_i^{*h}) - 2\rho k\varphi_2(\beth_m p_i^h, p_i^{*h}).
\end{aligned}
$$

Summing over $i = 1, 2, \ldots, j \leqslant N$ then results in,

$$
\begin{aligned}
&\|\boldsymbol{u}_j^h\|_V^2 + \|M^{-1/2} p_j^h\|_0^2 + \kappa \|\tau^{1/2} \boldsymbol{\varepsilon}_j^{*h}\|_0^2 + \vartheta \|\boldsymbol{\varepsilon}_j^{*h}\|_0^2 + (\varrho\varphi_0 + \rho\tau)\|p_j^{*h}\|_0^2 \\
&+ 2k \sum_{i=1}^{j} \left(\|K^{-1/2} \boldsymbol{z}_i^h\|_0^2 + \eta \|p_i^h\|_0^2 + \kappa \|\boldsymbol{\varepsilon}_i^{*h}\|_0^2 + \vartheta \|\tau^{1/2} \partial_t \boldsymbol{\varepsilon}_i^{*h}\|_0^2 + \varrho\tau \|\partial_t p_i^{*h}\|_0^2 + \rho\varphi_0 \|p_i^{*h}\|_0^2 \right) \\
&+ k^2 \sum_{i=1}^{j} \left(\|M^{-1/2} \partial_t p_i^h\|_0^2 + \|\partial_t \boldsymbol{u}_i^h\|_V^2 + \kappa \|\tau^{1/2} \partial_t \boldsymbol{\varepsilon}_i^{*h}\|_0^2 + \vartheta \|\partial_t \boldsymbol{\varepsilon}_i^{*h}\|_0^2 + (\varrho\varphi_0 + \rho\tau)\|\partial_t p_i^{*h}\|_0^2 \right) \\
&\qquad = -2\varrho k \varphi_2 \sum_{i=1}^{j} (\beth_m p_i^h, \partial_t p_i^{*h}) - 2\rho k \varphi_2 \sum_{i=1}^{j} (\beth_m p_i^h, p_i^{*h}) + 2k \sum_{i=1}^{j} (q_i, p_i^h) \\
&\qquad\quad + 2k \sum_{i=1}^{j} (\boldsymbol{f}_i, \partial_t \boldsymbol{u}_i^h) + 2k \sum_{i=1}^{j} (\boldsymbol{g}_i, \partial_t \boldsymbol{u}_i^h)_{\Gamma_N} + 2k \sum_{i=1}^{j} (\underline{\boldsymbol{\varepsilon}}_i^{*h}, \underline{\boldsymbol{\varepsilon}}(\partial_t \boldsymbol{u}_i^h)) \\
&\qquad + 2k\kappa \sum_{i=1}^{j} (\varphi_1 \underline{\boldsymbol{D}} \underline{\boldsymbol{\varepsilon}}(\beth_m \boldsymbol{u}_i^h), \boldsymbol{\varepsilon}_i^{*h}) + 2k\vartheta \sum_{i=1}^{j} (\varphi_1 \underline{\boldsymbol{D}} \underline{\boldsymbol{\varepsilon}}(\beth_m \boldsymbol{u}_i^h), \partial_t \boldsymbol{\varepsilon}_i^{*h}) - 2k\zeta \sum_{i=1}^{j} (p_i^h, p_i^{*h}).
\end{aligned}
$$

We now number the terms on the right as I, II, $\ldots$, IX and will consider them in smaller groups. Also since terms I and II contain the lagging operator we will leave them until after we have dealt with terms VII and $VIII$. To begin, and recalling that the initial data are zero, for term III we have,

$$
\begin{aligned}
2k \sum_{i=1}^{j} (q_i, p_i^h) &= 2k^2 \sum_{i=1}^{j} (q_i, \partial_t p_i^h) + 2k \sum_{i=1}^{j-1} (q_{i+1}, p_i^h) \\
&\leqslant (2k+1)k \sum_{i=1}^{j} \|M^{1/2} q_i\|_0^2 + k \sum_{i=1}^{j-1} \|M^{-1/2} p_i^h\|_0^2 + \frac{k^2}{2} \sum_{i=1}^{j} \|M^{-1/2} \partial_t p_i^h\|_0^2. \qquad (23)
\end{aligned}
$$

Note that this manipulation has meant that we do not have to assume that k is small enough in order to take the term in p_j^h to the left hand side. In fact term one on the right of this is bounded by data, the second can be handled with a discrete Gronwall lemma and the third will be kicked back — without requiring $\eta > 0$.

For terms IV and V we first note the following discrete-integration-by-parts identity for an arbitrary linear form, L,

$$
k \sum_{i=1}^{j} \Big(\langle L_i, \partial_t w_i \rangle + \langle \partial_t L_i, w_{i-1} \rangle \Big) = \langle L_j, w_j \rangle - \langle L_0, w_0 \rangle.
$$

Then, for IV and V we have,

$$
\begin{aligned}
2k \sum_{i=1}^{j} (\boldsymbol{f}_i, \partial_t \boldsymbol{u}_i^h) + 2k \sum_{i=1}^{j} (\boldsymbol{g}_i, \partial_t \boldsymbol{u}_i^h)_{\Gamma_N} &= 2(\boldsymbol{f}_j, \boldsymbol{u}_j^h) - 2(\boldsymbol{f}_0, \boldsymbol{u}_0^h) - 2k \sum_{i=1}^{j} (\partial_t \boldsymbol{f}_i, \boldsymbol{u}_{i-1}^h) \\
&\quad + 2(\boldsymbol{g}_j, \boldsymbol{u}_j^h)_{\Gamma_N} - 2(\boldsymbol{g}_0, \boldsymbol{u}_0^h)_{\Gamma_N} - 2k \sum_{i=1}^{j} (\partial_t \boldsymbol{g}_i, \boldsymbol{u}_{i-1}^h)_{\Gamma_N}, \\
&\leqslant \frac{1}{\epsilon_4} \|\boldsymbol{f}\|_{L_\infty(0,t_j;V')}^2 + \|\dot{\boldsymbol{f}}\|_{L_2(0,t_j;V')}^2 + \frac{C}{\epsilon_5} \|\boldsymbol{g}\|_{L_\infty(0,t_j;\boldsymbol{L}_2(\Gamma_N))}^2 + C \|\dot{\boldsymbol{g}}\|_{L_2(0,t_j;\boldsymbol{L}_2(\Gamma_N))}^2 \\
&\quad + (\epsilon_4 + \epsilon_5) \|\boldsymbol{u}_j^h\|_V^2 + 2k \sum_{i=1}^{j-1} \|\boldsymbol{u}_i^h\|_V^2,
\end{aligned}
$$

where we used a trace inequality and noted that since $\partial_t \boldsymbol{f}_i = k^{-1}\int_{t_{i-1}}^{t_i} \dot{\boldsymbol{f}}(s)\,ds$ we have

$$2k\sum_{i=1}^{j}(\partial_t \boldsymbol{f}_i, \boldsymbol{u}_{i-1}^h) \leqslant \int_0^{t_j} \|\dot{\boldsymbol{f}}(s)\|_{V'}^2\,ds + k\sum_{i=1}^{j}\|\boldsymbol{u}_{i-1}^h\|_V^2$$

with a similar estimate for the term in $\boldsymbol{g}$. Choosing $\epsilon_4 = \epsilon_5 = 1/4$ and putting these results together then gives,

$$\begin{aligned}
&\frac{1}{2}\|\boldsymbol{u}_j^h\|_V^2 + \|M^{-1/2}p_j^h\|_0^2 + \kappa\|\tau^{1/2}\underline{\boldsymbol{\sigma}}_j^{*h}\|_0^2 + \vartheta\|\underline{\boldsymbol{\sigma}}_j^{*h}\|_0^2 + (\varrho\varphi_0 + \rho\tau)\|p_j^{*h}\|_0^2 \\
&+ 2k\sum_{i=1}^{j}\left(\|K^{-1/2}\boldsymbol{z}_i^h\|_0^2 + \eta\|p_i^h\|_0^2 + \kappa\|\underline{\boldsymbol{\sigma}}_i^{*h}\|_0^2 + \vartheta\|\tau^{1/2}\partial_t\underline{\boldsymbol{\sigma}}_i^{*h}\|_0^2 + \varrho\tau\|\partial_t p_i^{*h}\|_0^2 + \rho\varphi_0\|p_i^{*h}\|_0^2\right) \\
&+ k^2\sum_{i=1}^{j}\left(\frac{\|M^{-1/2}\partial_t p_i^h\|_0^2}{2} + \|\partial_t\boldsymbol{u}_i^h\|_V^2 + \kappa\|\tau^{1/2}\partial_t\underline{\boldsymbol{\sigma}}_i^{*h}\|_0^2 + \vartheta\|\partial_t\underline{\boldsymbol{\sigma}}_i^{*h}\|_0^2 + (\varrho\varphi_0 + \rho\tau)\|\partial_t p_i^{*h}\|_0^2\right) \\
&\leqslant (2k+1)k\sum_{i=1}^{j}\|M^{1/2}q_i\|_0^2 + C\|\boldsymbol{f}\|_{H^1(0,t_j;V')}^2 + C\|\boldsymbol{g}\|_{H^1(0,t_j;\boldsymbol{L}_2(\Gamma_N))}^2 \\
&+ k\sum_{i=1}^{j-1}\left(\|M^{-1/2}p_i^h\|_0^2 + 2\|\boldsymbol{u}_i^h\|_V^2\right) + 2k\sum_{i=1}^{j}(\underline{\boldsymbol{\sigma}}_i^{*h}, \underline{\boldsymbol{\varepsilon}}(\partial_t\boldsymbol{u}_i^h)) + 2k\kappa\sum_{i=1}^{j}(\varphi_1\underline{\boldsymbol{D}}\underline{\boldsymbol{\varepsilon}}(\beth_m\boldsymbol{u}_i^h), \underline{\boldsymbol{\sigma}}_i^{*h}) \\
&+ 2k\vartheta\sum_{i=1}^{j}(\varphi_1\underline{\boldsymbol{D}}\underline{\boldsymbol{\varepsilon}}(\beth_m\boldsymbol{u}_i^h), \partial_t\underline{\boldsymbol{\sigma}}_i^{*h}) - 2\varrho k\varphi_2\sum_{i=1}^{j}(\beth_m p_i^h, \partial_t p_i^{*h}) \\
&- 2\rho k\varphi_2\sum_{i=1}^{j}(\beth_m p_i^h, p_i^{*h}) - 2k\zeta\sum_{i=1}^{j}(p_i^h, p_i^{*h}).
\end{aligned} \tag{24}$$

Now we label the last six terms as A, B, C, D, E and F and continue. First, since $\boldsymbol{u}(0) = \boldsymbol{0}$ and $\underline{\boldsymbol{\sigma}}_0^{*h} = \underline{\boldsymbol{0}}$ we get for term A that,

$$\begin{aligned}
&2k\sum_{i=1}^{j}(\underline{\boldsymbol{\sigma}}_i^{*h}, \underline{\boldsymbol{\varepsilon}}(\partial_t\boldsymbol{u}_i^h)) = 2(\underline{\boldsymbol{\sigma}}_j^{*h}, \underline{\boldsymbol{\varepsilon}}(\boldsymbol{u}_j^h)) - 2k\sum_{i=1}^{j}(\partial_t\underline{\boldsymbol{\sigma}}_i^{*h}, \underline{\boldsymbol{\varepsilon}}(\boldsymbol{u}_{i-1}^h)) \\
&\leqslant \epsilon_A\|\boldsymbol{u}_j^h\|_V^2 + \frac{\|\underline{\boldsymbol{D}}^{-1}\|_{\underline{\boldsymbol{L}}_\infty(\Omega)}}{\epsilon_A}\|\underline{\boldsymbol{\sigma}}_j^{*h}\|_0^2 + \epsilon'_A k\sum_{i=1}^{j}\|\tau^{1/2}\partial_t\underline{\boldsymbol{\sigma}}_i^{*h}\|_0^2 + \frac{k}{\epsilon'_A}\sum_{i=1}^{j-1}\frac{\|\underline{\boldsymbol{D}}^{-1}\|_{\underline{\boldsymbol{L}}_\infty(\Omega)}}{\tau}\|\boldsymbol{u}_i^h\|_V^2.
\end{aligned}$$

In this the last term can be handled with a Gronwall inequality but the other three terms have to be kicked-back. For term F we have

$$2k\zeta\sum_{i=1}^{j}(p_i^h, p_i^{*h}) \leqslant k\zeta\epsilon_F\sum_{i=1}^{j}\|p_i^h\|_0^2 + \frac{k\zeta}{\epsilon_F}\sum_{i=1}^{j}\|p_i^{*h}\|_0^2$$

for every $\epsilon_F > 0$.

Terms B and C both contain the lagging operator so we deal first with the lagged case where $m = 1$ and $\beth_1\boldsymbol{u}_i^h := \boldsymbol{u}_{i-1}^h$. Again using $\boldsymbol{u}(0) = \boldsymbol{0}$ for term B we then have,

$$2k\kappa\sum_{i=1}^{j}(\varphi_1\underline{\boldsymbol{D}}\underline{\boldsymbol{\varepsilon}}(\boldsymbol{u}_{i-1}^h), \underline{\boldsymbol{\sigma}}_i^{*h}) \leqslant k\kappa\sum_{i=1}^{j}\|\underline{\boldsymbol{\sigma}}_i^{*h}\|_0^2 + k\kappa\sum_{i=1}^{j-1}\varphi_1^2\|\underline{\boldsymbol{D}}\|_{\underline{\boldsymbol{L}}_\infty(\Omega)}\|\boldsymbol{u}_i^h\|_V^2,$$

while for term C,

$$2k\vartheta\sum_{i=1}^{j}(\varphi_1\underline{\boldsymbol{D}}\underline{\boldsymbol{\varepsilon}}(\boldsymbol{u}_{i-1}^h),\partial_t\underline{\boldsymbol{\sigma}}_i^{*h})\leqslant k\vartheta\sum_{i=1}^{j}\|\tau^{1/2}\partial_t\underline{\boldsymbol{\sigma}}_i^{*h}\|_0^2+k\vartheta\sum_{i=1}^{j-1}\frac{\varphi_1^2}{\tau}\|\underline{\boldsymbol{D}}\|_{\underline{\boldsymbol{L}}_\infty(\Omega)}\|\boldsymbol{u}_i^h\|_V^2.$$

For terms D and E in the lagged case and with $\varrho=1$ we have,

$$\begin{aligned}2k\varphi_2\sum_{i=1}^{j}(p_{i-1}^h,\partial_t p_i^{*h})+2k\rho\varphi_2\sum_{i=1}^{j}(p_{i-1}^h,p_i^{*h})&\leqslant\left(\frac{\rho}{\varphi_0}+\frac{1}{\tau}\right)k\varphi_2^2M\sum_{i=1}^{j-1}\|M^{-1/2}p_i^h\|_0^2\\&\quad+2k\sum_{i=1}^{j}\left(\frac{\tau}{2}\|\partial_t p_i^{*h}\|_0^2+\frac{\rho\varphi_0}{2}\|p_i^{*h}\|_0^2\right).\end{aligned}$$

Merging these into (24) then results in,

$$\begin{aligned}&\left(\frac{1}{2}-\epsilon_A\right)\|\boldsymbol{u}_j^h\|_V^2+\|M^{-1/2}p_j^h\|_0^2+\kappa\|\tau^{1/2}\underline{\boldsymbol{\sigma}}_j^{*h}\|_0^2+\left(\vartheta-\frac{\|\underline{\boldsymbol{D}}^{-1}\|_{\underline{\boldsymbol{L}}_\infty(\Omega)}}{\epsilon_A}\right)\|\underline{\boldsymbol{\sigma}}_j^{*h}\|_0^2\\&\quad+(\varphi_0+\rho\tau)\|p_j^{*h}\|_0^2+2k\sum_{i=1}^{j}\left(\|K^{-1/2}\boldsymbol{z}_i^h\|_0^2+\left(\eta-\frac{\zeta\epsilon_F}{2}\right)\|p_i^h\|_0^2+\frac{\kappa}{2}\|\underline{\boldsymbol{\sigma}}_i^{*h}\|_0^2\right.\\&\quad\left.+\frac{\vartheta-\epsilon_A'}{2}\|\tau^{1/2}\partial_t\underline{\boldsymbol{\sigma}}_i^{*h}\|_0^2+\frac{\tau}{2}\|\partial_t p_i^{*h}\|_0^2+\frac{1}{2}\left(\rho\varphi_0-\frac{\zeta}{\epsilon_F}\right)\|p_i^{*h}\|_0^2\right)\\&\quad+k^2\sum_{i=1}^{j}\left(\frac{1}{2}\|M^{-1/2}\partial_t p_i^h\|_0^2+\|\partial_t\boldsymbol{u}_i^h\|_V^2+\vartheta\|\partial_t\underline{\boldsymbol{\sigma}}_i^{*h}\|_0^2\right.\\&\quad\left.+\kappa\|\tau^{1/2}\partial_t\underline{\boldsymbol{\sigma}}_i^{*h}\|_0^2+(\varphi_0+\rho\tau)\|\partial_t p_i^{*h}\|_0^2\right)\\&\leqslant C\|\boldsymbol{f}\|_{H^1(0,t_j;V')}^2+C\|\boldsymbol{g}\|_{H^1(0,t_j;\boldsymbol{L}_2(\Gamma_N))}^2+(2k+1)k\sum_{i=1}^{j}\|M^{1/2}q_i\|_0^2\\&\quad+Ck\sum_{i=1}^{j-1}\left(\|M^{-1/2}p_i^h\|_0^2+\left(1+\kappa+\vartheta+\frac{1}{\epsilon_A'}\right)\|\boldsymbol{u}_i^h\|_V^2\right).\end{aligned}$$

Next, recalling that we are assuming $\varphi_1>0$, we choose ρ large enough so that $\rho>\zeta\tau/2\varphi_0\varphi_1$. Therefore $\zeta/\varphi_0\rho<2\varphi_1/\tau$ and we can find ϵ_F so that $\zeta/\varphi_0\rho<\epsilon_F<2\varphi_1/\tau$. Recalling that $\eta=\zeta\varphi_1/\tau$ we can conclude that $\epsilon_F<2\eta/\zeta$ or, in the more relevant form, $\eta-\epsilon_F\zeta/2>0$. On the other hand we also see that $\zeta/\varphi_0\rho<\epsilon_F$ implies $\zeta/\epsilon_F<\varphi_0\rho$ or, what is again more relevant, $\varphi_0\rho-\zeta/\epsilon_F>0$. Lastly we choose (for example) $\epsilon_A=1/3$, $\kappa=2$, $\vartheta=2\epsilon_A'$ with $\epsilon_A'=2\|\underline{\boldsymbol{D}}^{-1}\|_{\underline{\boldsymbol{L}}_\infty(\Omega)}$ and apply Gronwall's inequality to give the desired result (which is uniform in ζ) for any time step $k>0$.

Turning now to the non-lagged case we have $m=0$ and $\beth_0\boldsymbol{u}_i^h:=\boldsymbol{u}_i^h$. In this case for term

B we have,

$$2k\kappa\sum_{i=1}^{j}(\varphi_1\underline{\boldsymbol{D}}\underline{\boldsymbol{\varepsilon}}(\boldsymbol{u}_i^h),\underline{\boldsymbol{\sigma}}_i^{*h})=2k^2\kappa\sum_{i=1}^{j}(\varphi_1\underline{\boldsymbol{D}}\underline{\boldsymbol{\varepsilon}}(\partial_t\boldsymbol{u}_i^h),\underline{\boldsymbol{\sigma}}_i^{*h})+2k\kappa\sum_{i=0}^{j-1}(\varphi_1\underline{\boldsymbol{D}}\underline{\boldsymbol{\varepsilon}}(\boldsymbol{u}_i^h),\underline{\boldsymbol{\sigma}}_{i+1}^{*h})$$
$$\leqslant\epsilon_B k^2\kappa^2\varphi_1^2\|\underline{\boldsymbol{D}}\|_{\underline{\boldsymbol{L}}_\infty(\Omega))}\sum_{i=1}^{j}\|\partial_t\boldsymbol{u}_i^h\|_V^2+\frac{k^2}{\epsilon_B}\sum_{i=1}^{j}\|\underline{\boldsymbol{\sigma}}_i^{*h}\|_0^2$$
$$+\epsilon'_B k\kappa\sum_{i=1}^{j}\|\underline{\boldsymbol{\sigma}}_i^{*h}\|_0^2+\frac{k\kappa\varphi_1^2\|\underline{\boldsymbol{D}}\|_{\underline{\boldsymbol{L}}_\infty(\Omega))}}{\epsilon'_B}\sum_{i=1}^{j-1}\|\boldsymbol{u}_i^h\|_V^2.$$

The last term on the right can be 'Gronwalled' but the others will be kicked-back. Next, for term C we obtain,

$$2k\vartheta\sum_{i=1}^{j}(\varphi_1\underline{\boldsymbol{D}}\underline{\boldsymbol{\varepsilon}}(\boldsymbol{u}_i^h),\partial_t\underline{\boldsymbol{\sigma}}_i^{*h})=2k^2\vartheta\sum_{i=1}^{j}(\varphi_1\underline{\boldsymbol{D}}\underline{\boldsymbol{\varepsilon}}(\partial_t\boldsymbol{u}_i^h),\partial_t\underline{\boldsymbol{\sigma}}_i^{*h})+2k\vartheta\sum_{i=0}^{j-1}(\varphi_1\underline{\boldsymbol{D}}\underline{\boldsymbol{\varepsilon}}(\boldsymbol{u}_i^h),\partial_t\underline{\boldsymbol{\sigma}}_{i+1}^{*h})$$
$$\leqslant\frac{k^2}{\tau\epsilon_C}\sum_{i=1}^{j}\|\tau^{1/2}\partial_t\underline{\boldsymbol{\sigma}}_i^{*h}\|_0^2+\epsilon_C k^2\vartheta^2\varphi_1^2\|\underline{\boldsymbol{D}}\|_{\underline{\boldsymbol{L}}_\infty(\Omega))}\sum_{i=1}^{j}\|\partial_t\boldsymbol{u}_i^h\|_V^2$$
$$+\frac{k\vartheta}{\epsilon'_C}\sum_{i=1}^{j-1}\frac{\varphi_1^2\|\underline{\boldsymbol{D}}\|_{\underline{\boldsymbol{L}}_\infty(\Omega))}}{\tau}\|\boldsymbol{u}_i^h\|_V^2+\epsilon'_C k\vartheta\sum_{i=1}^{j}\|\tau^{1/2}\partial_t\underline{\boldsymbol{\sigma}}_i^{*h}\|_0^2,$$

while for D we have

$$2\varrho k\varphi_2\sum_{i=1}^{j}(p_i^h,\partial_t p_i^{*h})=2\varrho k^2\varphi_2\sum_{i=1}^{j}(\partial_t p_i^h,\partial_t p_i^{*h})+2\varrho k\varphi_2\sum_{i=1}^{j}(p_{i-1}^h,\partial_t p_i^{*h})$$
$$\leqslant\sum_{i=1}^{j}\left(\frac{k^2}{\epsilon_D}+k\varrho\epsilon'_D\right)\|\partial_t p_i^{*h}\|_0^2+k^2\sum_{i=1}^{j}\epsilon_D\varrho^2\varphi_2^2M\|M^{-1/2}\partial_t p_i^h\|_0^2+\frac{\varrho M\varphi_2^2k}{\epsilon'_D}\sum_{i=1}^{j-1}\|M^{-1/2}p_i^h\|_0^2$$

for every $\epsilon_D,\epsilon'_D>0$. Lastly, for E,

$$2\rho k\varphi_2\sum_{i=1}^{j}(p_i^h,p_i^{*h})=2\rho k^2\varphi_2\sum_{i=1}^{j}(\partial_t p_i^h,p_i^{*h})+2\rho k\varphi_2\sum_{i=1}^{j}(p_{i-1}^h,p_i^{*h})$$
$$\leqslant\sum_{i=1}^{j}\left(\frac{k^2\varphi_0}{\epsilon_E}+\epsilon'_E k\rho\varphi_0\right)\|p_i^{*h}\|_0^2+k^2\sum_{i=1}^{j}\frac{\epsilon_E\rho^2\varphi_2^2M}{\varphi_0}\|M^{-1/2}\partial_t p_i^h\|_0^2$$
$$+\frac{\rho\varphi_2^2Mk}{\varphi_0\epsilon'_E}\sum_{i=1}^{j-1}\|M^{-1/2}p_i^h\|_0^2$$

for every $\epsilon_E,\epsilon'_E>0$.

Assembling these results into (24) now gives,

$$\left(\frac{1}{2}-\epsilon_A\right)\|\boldsymbol{u}_j^h\|_V^2+\|M^{-1/2}p_j^h\|_0^2+\kappa\|\tau^{1/2}\underline{\boldsymbol{\sigma}}_j^{*h}\|_0^2+\left(\vartheta-\frac{\|\underline{\boldsymbol{D}}^{-1}\|_{\underline{\boldsymbol{L}}_\infty(\Omega)}}{\epsilon_A}\right)\|\underline{\boldsymbol{\sigma}}_j^{*h}\|_0^2$$
$$+(\varrho\varphi_0+\rho\tau)\|p_j^{*h}\|_0^2+2k\left(\eta-\frac{\zeta\epsilon_F}{2}\right)\sum_{i=1}^{j}\|p_i^h\|_0^2+2k\sum_{i=1}^{j}\|K^{-1/2}\boldsymbol{z}_i^h\|_0^2$$
$$+k^2\left(\frac{1}{2}-\epsilon_D\varrho^2\varphi_2^2M-\frac{\epsilon_E\rho^2\varphi_2^2M}{\varphi_0}\right)\sum_{i=1}^{j}\|M^{-1/2}\partial_t p_i^h\|_0^2+\kappa k^2\sum_{i=1}^{j}\|\tau^{1/2}\partial_t\underline{\boldsymbol{\sigma}}_i^{*h}\|_0^2$$
$$+\left((2\tau-\epsilon'_D)\varrho-\frac{k}{\epsilon_D}\right)k\sum_{i=1}^{j}\|\partial_t p_i^{*h}\|_0^2+2k\left(\rho\varphi_0-\frac{\zeta}{2\epsilon_F}-\frac{k\varphi_0}{2\epsilon_E}-\frac{\epsilon'_E\rho\varphi_0}{2}\right)\sum_{i=1}^{j}\|p_i^{*h}\|_0^2$$
$$+k^2(\varrho\varphi_0+\rho\tau)\sum_{i=1}^{j}\|\partial_t p_i^{*h}\|_0^2+\left((2-\epsilon'_C)\vartheta-\epsilon'_A-\frac{k}{\tau\epsilon_C}\right)k\sum_{i=1}^{j}\|\tau^{1/2}\partial_t\underline{\boldsymbol{\sigma}}_i^{*h}\|_0^2$$
$$+\left((2-\epsilon'_B)\kappa-\frac{k}{\epsilon_B}\right)k\sum_{i=1}^{j}\|\underline{\boldsymbol{\sigma}}_i^{*h}\|_0^2$$
$$+\Big(1-(\epsilon_B\kappa^2+\epsilon_C\vartheta^2)\varphi_1^2\|\underline{\boldsymbol{D}}\|_{\underline{\boldsymbol{L}}_\infty(\Omega))}\Big)k^2\sum_{i=1}^{j}\|\partial_t\boldsymbol{u}_i^h\|_V^2$$
$$+\vartheta k^2\sum_{i=1}^{j}\|\partial_t\underline{\boldsymbol{\sigma}}_i^{*h}\|_0^2\leqslant(2k+1)k\sum_{i=1}^{j}\|M^{1/2}q_i\|_0^2+C\|\boldsymbol{f}\|^2_{H^1(0,t_j;V')}+C\|\boldsymbol{g}\|^2_{H^1(0,t_j;\boldsymbol{L}_2(\Gamma_N))}$$
$$+k\sum_{i=1}^{j-1}\Bigg(\left(1+\frac{\rho\varphi_2^2M}{\varphi_0\epsilon'_E}+\frac{\varrho M\varphi_2^2}{\epsilon'_D}\right)\|M^{-1/2}p_i^h\|_0^2$$
$$+\left(2+\frac{\|\underline{\boldsymbol{D}}^{-1}\|_{\underline{\boldsymbol{L}}_\infty(\Omega))}}{\tau\epsilon'_A}+\left(\frac{\kappa}{\epsilon'_B}+\frac{\vartheta}{\tau\epsilon'_C}\right)\varphi_1^2\|\underline{\boldsymbol{D}}\|_{\underline{\boldsymbol{L}}_\infty(\Omega))}\right)\|\boldsymbol{u}_i^h\|_V^2\Bigg).$$

The next step is to choose the ϵ's so as to keep all of the coefficients on the left positive. We begin this procedure by dealing first with the terms involving p^h and p^{*h}.

First we see that ϵ'_E and ϵ'_D can be chosen rather freely since they appear in the summation on the right hand side so, to simplify the arguments that are coming, we will take $\epsilon'_E=1$ and insist that $\epsilon'_D<2\tau$ which is possible since $\tau>0$. With this we observe that $\varrho\varphi_0+\rho\tau>0$ by assumption and that, since $\eta=\zeta\varphi_1/\tau>0$ (recall that $\varphi_1>0$), we can guarantee that $\eta-\zeta\epsilon_F/2>0$ by insisting that $\epsilon_F<2\varphi_1/\tau$. In a similar vein we can guarantee that $(2\tau-\epsilon'_D)\varrho-k/\epsilon_D>0$ by insisting that $\epsilon_D>k/((2\tau-\epsilon'_D)\varrho)$ which (recalling that $2\tau-\epsilon'_D>0$) is always achievable by controlling k/ϱ.

Now, since $\epsilon'_E=1$ we see that

$$\rho\varphi_0-\frac{\zeta}{2\epsilon_F}-\frac{k\varphi_0}{2\epsilon_E}-\frac{\epsilon'_E\rho\varphi_0}{2}>0\qquad\Longleftrightarrow\qquad\rho\varphi_0-\frac{\zeta}{\epsilon_F}-\frac{k\varphi_0}{\epsilon_E}>0$$

which, in turn, is equivalent to $\epsilon_E>\epsilon_F k\varphi_0/(\rho\varphi_0\epsilon_F-\zeta)$ which can be guaranteed by choosing k small enough with the proviso that $\rho\varphi_0\epsilon_F-\zeta>0$, or $\epsilon_F>\zeta/\rho\varphi_0$. Taken together with the earlier restriction on ϵ_F we have therefore to require that,

$$\frac{\zeta}{\rho\varphi_0}<\epsilon_F<\frac{2\varphi_1}{\tau}$$

which is always achievable by choosing ρ large enough. The last of this set of terms to be concerned about is the requirement that

$$\frac{1}{2} - \epsilon_D \varrho^2 \varphi_2^2 M - \frac{\epsilon_E \rho^2 \varphi_2^2 M}{\varphi_0} > 0$$

which, with the lower bounds on ϵ_D and ϵ_E stated above, can be re-written and bounded as,

$$\frac{1}{2M} > \epsilon_D \varrho^2 \varphi_2^2 + \frac{\epsilon_E \rho^2 \varphi_2^2}{\varphi_0} > \frac{k\varrho\varphi_2^2}{(2\tau - \epsilon'_D)} + \frac{k\epsilon_F \rho^2 \varphi_2^2}{\rho\varphi_0\epsilon_F - \zeta}.$$

This can always be achieved by requiring small enough time step k and so with any $\varrho > 0$ completes the calculations regarding the internal viscous pressure variables.

Turning now to the terms involving $\boldsymbol{\varrho}^{*h}$ we notice this time that ϵ'_A, ϵ'_B and ϵ'_C can be chosen freely since they are balanced on the right by the 'Gronwall coefficient', and we recall that we are still free to choose $\kappa, \vartheta > 0$.

Clearly we need to insist that $\epsilon_A < 1/2$ with $\vartheta - \|\underline{\boldsymbol{D}}^{-1}\|_{\underline{\boldsymbol{L}}_\infty(\Omega)}/\epsilon_A > 0$ simultaneously. Hence we require that $\epsilon_A > \vartheta^{-1}\|\underline{\boldsymbol{D}}^{-1}\|_{\underline{\boldsymbol{L}}_\infty(\Omega)}$ and so such an $\epsilon_A > 0$ exists by insisting that $\vartheta > 2\|\underline{\boldsymbol{D}}^{-1}\|_{\underline{\boldsymbol{L}}_\infty(\Omega)}$. Now, for some $\epsilon \in (0,1)$ we set $\epsilon'_A = \epsilon\vartheta$ and $\epsilon'_C = \epsilon$ and then $(2 - \epsilon'_C)\vartheta - \epsilon'_A - k/\tau\epsilon_C > 0$ will be guaranteed if we insist that $\epsilon_C > k/((2-2\epsilon)\vartheta\tau)$.

In a similar vein, if $\epsilon'_B \in (0,2)$ then $(2 - \epsilon'_B)\kappa - k/\epsilon_B > 0$ is guaranteed by $\epsilon_B > k/[(2-\epsilon'_B)\kappa]$. Clearly ϵ'_A, ϵ'_B and ϵ'_C can all be chosen within these constraints and so, even with the lower bound on ϑ, we have derived achievable lower bounds on ϵ_B and ϵ_C and a non-empty two-sided bound on ϵ_A. The last requirement is that,

$$1 - (\epsilon_B\kappa^2 + \epsilon_C\vartheta^2)\varphi_1^2\|\underline{\boldsymbol{D}}\|_{\underline{\boldsymbol{L}}_\infty(\Omega)} > 0 \qquad \text{or, equivalently,}$$
$$\epsilon_B\kappa^2 + \epsilon_C\vartheta^2 < \frac{1}{\varphi_1^2\|\underline{\boldsymbol{D}}\|_{\underline{\boldsymbol{L}}_\infty(\Omega)}}.$$

Observing the lower bounds on ϵ_B and ϵ_C we also need,

$$\epsilon_B\kappa^2 + \epsilon_C\vartheta^2 > \frac{k\kappa}{2 - \epsilon'_B} + \frac{k\vartheta}{(2-2\epsilon)\tau}.$$

Putting these last two inequalities together and using the lower bound on ϑ then results in,

$$\frac{1}{\varphi_1^2\|\underline{\boldsymbol{D}}\|_{\underline{\boldsymbol{L}}_\infty(\Omega)}} > \left(\frac{\kappa}{2-\epsilon'_B} + \frac{\vartheta}{(2-2\epsilon)\tau}\right)k > \left(\frac{\kappa}{2-\epsilon'_B} + \frac{\|\underline{\boldsymbol{D}}^{-1}\|_{\underline{\boldsymbol{L}}_\infty(\Omega)}}{(1-\epsilon)\tau}\right)k$$

and this will be satisfied if k is small enough. Therefore, for small enough time step, the proof is completed by using the discrete Gronwall lemma.

Remark 3.3 *Note that the six terms labelled A, ..., F in* (24) *are not present in poroelasticity and the inequality then reflects the unconditional* (*in terms of time step*) *stability of the coupled poroelasticity algorithm.*

On the other hand the time step restriction in the non-lagged algorithm seems to be necessary. If we note that sending $\varphi_1 \to 0$ or $\tau \to \infty$, both representing the vanishing of viscoelasticity, then by examining the proof we can see that the restriction on the time step vanishes and we get back to the unconditional stability of poroelasticity. This suggests that not too much information has been discarded in the foregoing analysis.

Since the problem is linear we have a well-posedness result for the discrete schemes.

Proposition 3.4 (discrete well-posedness) *Assume* (12). *Then* (*for small enough time step in the case of* $\exists_0$) *the discrete problem has a unique solution that depends continuously on the data.*

Proof. The initial data are zero and for each time step, given unique previous values, the discrete scheme defines a linear map from the data into the discrete solution space. The stability estimate implies that this map is bijective. ∎

4 Error estimates

We now move on to explore the convergence properties of the lagged scheme and derive an *a priori* error bound. To begin we introduce projections,

$$\begin{aligned} &\Pi_p \colon L_2(\Omega) \to W^h, && \Pi_z \colon \boldsymbol{H}_0(\mathrm{div};\Omega) \to \mathrm{RT}^h, \\ &\Pi_u \colon V \to V^h, && \Pi_\sigma \colon \underline{\boldsymbol{L}}_2(\Omega) \to \underline{\boldsymbol{W}}^h, \end{aligned}$$

as follows. Π_p and Π_σ are defined as the standard $L_2(\Omega)$ and $\underline{\boldsymbol{L}}_2(\Omega)$ projections; Π_u is the usual Ritz, or elliptic, projection defined through $a(\cdot,\cdot)$; and, Π_z is the usual Raviart-Thomas interpolator, see [23], which satisfies $(\nabla\cdot(\boldsymbol{w}-\Pi_z\boldsymbol{w}),\phi)=0$ for all $\phi\in W^h$ and for which $\|\boldsymbol{w}-\Pi_z\boldsymbol{w}\|_0 \leqslant Ch\|\boldsymbol{w}\|_1$.

Defining the error components,

$$\begin{aligned} E_p^i &:= p_i^h - \Pi_p p(t_i), & \mathscr{E}_p(t) &:= p(t) - \Pi_p p(t), \\ E_z^i &:= \boldsymbol{z}_i^h - \Pi_z \boldsymbol{z}(t_i), & \mathscr{E}_z(t) &:= \boldsymbol{z}(t) - \Pi_z \boldsymbol{z}(t), \\ E_u^i &:= \boldsymbol{u}_i^h - \Pi_u \boldsymbol{u}(t_i), & \mathscr{E}_u(t) &:= \boldsymbol{u}(t) - \Pi_u \boldsymbol{u}(t), \\ E_\sigma^i &:= \underline{\boldsymbol{\sigma}}_i^{*h} - \Pi_\sigma \underline{\boldsymbol{\sigma}}^*(t_i), & \mathscr{E}_\sigma(t) &:= \underline{\boldsymbol{\sigma}}^*(t) - \Pi_\sigma \underline{\boldsymbol{\sigma}}^*(t), \\ E_c^i &:= p_i^{*h} - \Pi_p p^*(t_i), & \mathscr{E}_c(t) &:= p^*(t) - \Pi_p p^*(t), \end{aligned}$$

so that $p_i^h - p(t_i) = E_p^i - \mathscr{E}_p(t_i)$ and so on, the error bound will follow in the usual way by first bounding the 'E' quantities in terms of the approximation errors embodied in the '$\mathscr{E}$' quantities and the finite difference approximations, and then using the triangle inequality.

The approximation-error bound,

$$\begin{aligned} \|\mathscr{E}_\sigma\|_{W_\infty^1(I;\underline{\boldsymbol{L}}_2(\Omega))} + \|\mathscr{E}_u\|_{W_\infty^1(I;V)} + \|\mathscr{E}_p\|_{W_\infty^1(I;L_2(\Omega))} + \|\mathscr{E}_z\|_{L_\infty(I;\boldsymbol{L}_2(\Omega))} + \|\mathscr{E}_c\|_{W_\infty^1(I;\boldsymbol{L}_2(\Omega))} \\ \leqslant Ch\Big(\|\underline{\boldsymbol{\sigma}}^*\|_{W_\infty^1(I;\underline{\boldsymbol{H}}^1(\Omega))} + \|\boldsymbol{u}\|_{W_\infty^1(I;\underline{\boldsymbol{H}}^2(\Omega))} + \|p\|_{W_\infty^1(I;\underline{\boldsymbol{H}}^1(\Omega))} \\ + \|p\|_{L_\infty(I;\underline{\boldsymbol{H}}^2(\Omega))} + \|p^*\|_{W_\infty^1(I;\underline{\boldsymbol{H}}^2(\Omega))} \Big), \end{aligned} \tag{25}$$

follows by standard results, and we note from (1) and (6) that $\underline{\boldsymbol{\sigma}}^* \in W_p^{m+1}(I;\underline{\boldsymbol{H}}^1(\Omega))$ whenever we have $\boldsymbol{u} \in W_p^m(I;\boldsymbol{H}^2(\Omega))$, and also that $p^* \in W_p^{m+1}(I;L_2(\Omega))$ whenever $p \in W_p^m(I;L_2(\Omega))$.

We now give the main technical argument that will contribute toward the *a priori* error bound below in Theorem 4.2.

Lemma 4.1 (main error bound) *Assume* (12) *along with,*

- $p \in L_\infty(I; H^2(\Omega)) \cap W^1_\infty(I; H^1(\Omega)) \cap H^2(I; L_2(\Omega))$*;*
- $\boldsymbol{u} \in W^1_\infty(I; \boldsymbol{H}^2(\Omega)) \cap H^2(I; V)$*;*
- $\boldsymbol{\sigma}^* \in W^1_\infty(I; \boldsymbol{H}^1(\Omega)) \cap H^2(I; \boldsymbol{L}_2(\Omega))$*;*
- $p^* \in W^2_2(I; L_2(\Omega))$*,*

then for the lagged scheme, with any time step $k > 0$,

$$\|M^{-1/2}E_p^j\|_0^2 + \|E_u^j\|_V^2 + \|E_\sigma^j\|_0^2 + \|\varphi_0^{1/2}E_c^j\|_0^2 + \sum_{i=1}^{j}\left(k\|K^{-1/2}E_z^i\|_0^2 + k\|\tau^{1/2}\partial_t E_\sigma^i\|_0^2 + k\|\tau^{1/2}\partial_t E_c^i\|_0^2\right) \leqslant Ck^2 + Ch^2$$

for a constant C independent of h and k.

Proof. The approach is quite standard and so we include only the main steps. Subtract each of (13), (14), (15), (16), (17) (at t_i) from its counterpart in (18), (19), (20), (21), (22) with the choices $\phi = E_p^i$, $\boldsymbol{\chi} = \partial_t E_u^i$, $\boldsymbol{\psi} = -E_z^i$, $\underline{\boldsymbol{\theta}} = \vartheta\partial_t E_\sigma^i$, for some $\vartheta > 0$, and $\varpi = \partial_t E_c^i$. Add the resulting equations, notice that the terms involving $(\alpha\nabla\cdot\partial_t E_u^i, E_p^i)$ and $(\nabla\cdot E_z^i, E_p^i)$ are self-eliminating, and multiply by $2k$ to get,

$$\begin{aligned}
&k\partial_t\|M^{-1/2}E_p^i\|_0^2 + k\partial_t\|E_u^i\|_V^2 + \vartheta k\partial_t\|E_\sigma^i\|_0^2 + k\partial_t\|\varphi_0^{1/2}E_c^i\|_0^2 + 2k\|\tau^{1/2}\partial_t E_c^i\|_0^2\\
&+ 2k\|K^{-1/2}E_z^i\|_0^2 + 2k\vartheta\|\tau^{1/2}\partial_t E_\sigma^i\|_0^2 + k^2\|M^{-1/2}\partial_t E_p^i\|_0^2 + k^2\|\varphi_0^{1/2}\partial_t E_c^i\|_0^2 + k^2\|\partial_t E_u^i\|_V^2\\
&+ \vartheta k^2\|\partial_t E_\sigma^i\|_0^2 = 2k(M^{-1}(\dot p(t_i) - \partial_t p_i), E_p^i) + 2k(\alpha\nabla\cdot(\dot{\boldsymbol{u}}(t_i) - \partial_t\boldsymbol{u}_i), E_p^i)\\
&+ 2k\vartheta(\tau\dot{\underline{\boldsymbol{\sigma}}}^*(t_i) - \tau\partial_t\underline{\boldsymbol{\sigma}}_i^*, \partial_t E_\sigma^i) - 2k\vartheta(\varphi_1\underline{\boldsymbol{D}}\underline{\boldsymbol{\varepsilon}}(\boldsymbol{u}_i - \boldsymbol{u}_{i-1}), \partial_t E_\sigma^i) + 2k(M^{-1}\partial_t\mathscr{E}_p(t_i), E_p^i)\\
&+2k(\nabla\cdot\mathscr{E}_z(t_i), E_p^i)+2k(\alpha\nabla\cdot\partial_t\mathscr{E}_u(t_i), E_p^i)+2k(K^{-1}\mathscr{E}_z(t_i), E_z^i)-2k\vartheta(\varphi_1\underline{\boldsymbol{D}}\underline{\boldsymbol{\varepsilon}}(\mathscr{E}_u(t_{i-1})), \partial_t E_\sigma^i)\\
&+ 2k\vartheta(\tau\partial_t\mathscr{E}_\sigma(t_i), \partial_t E_\sigma^i) + 2k\vartheta(\mathscr{E}_\sigma(t_i), \partial_t E_\sigma^i) + 2k\vartheta(\varphi_1\underline{\boldsymbol{D}}\underline{\boldsymbol{\varepsilon}}(E_u^{i-1}), \partial_t E_\sigma^i) - 2k(\mathscr{E}_p(t_i), \nabla\cdot E_z^i)\\
&+ 2ka(\mathscr{E}_u(t_i), \partial_t E_u^i) - 2k(\mathscr{E}_\sigma(t_i), \underline{\boldsymbol{\varepsilon}}(\partial_t E_u^i)) - 2k(\alpha\mathscr{E}_p(t_i), \nabla\cdot\partial_t E_u^i) + 2k(E_\sigma^i, \underline{\boldsymbol{\varepsilon}}(\partial_t E_u^i))\\
&- 2k(\varphi_2 E_p^{i-1}, \partial_t E_c^i) + 2k\tau(\dot p^*(t_i) - \partial_t p^*(t_i), \partial_t E_c^i) + 2k\varphi_2(p(t_i) - p(t_{i-1}), \partial_t E_c^i)\\
&+ 2k\tau(\partial_t\mathscr{E}_c(t_i), \partial_t E_c^i) + 2k\varphi_0(\mathscr{E}_c(t_i), \partial_t E_c^i) + 2k\varphi_2(\mathscr{E}_p(t_{i-1}), \partial_t E_c^i).
\end{aligned}$$

Now, in the right hand side of this, we observe the orthogonalities for

$$\begin{aligned}
\text{term 5}: &\quad (M^{-1}\partial_t\mathscr{E}_p(t_i), E_p^i) = 0;\\
\text{term 6}: &\quad (\nabla\cdot\mathscr{E}_z(t_i), E_p^i) = 0;\\
\text{term 10}: &\quad \vartheta(\tau\partial_t\mathscr{E}_\sigma(t_i), \partial_t E_\sigma^i) = 0;\\
\text{term 11}: &\quad \vartheta(\mathscr{E}_\sigma(t_i), \partial_t E_\sigma^i) = 0;\\
\text{term 13}: &\quad (\mathscr{E}_p(t_i), \nabla\cdot E_z^i) = 0 \quad (\text{since } \nabla\cdot E_z^i \in W^h\times W^h);\\
\text{term 14}: &\quad a(\mathscr{E}_u(t_i), \partial_t E_u^i) = 0;\\
\text{term 21}: &\quad (\partial_t\mathscr{E}_c(t_i), \partial_t E_c^i) = 0;\\
\text{term 22}: &\quad (\mathscr{E}_c(t_i), \partial_t E_c^i) = 0;\\
\text{term 23}: &\quad (\mathscr{E}_p(t_{i-1}), \partial_t E_c^i) = 0,
\end{aligned}$$

and so, upon removing right-hand-side terms 5, 6, 10, 11, 13, 14, 21, 22 and 23, we are left with,

$$
\begin{aligned}
&k\partial_t\|M^{-1/2}E_p^i\|_0^2+k\partial_t\|E_u^i\|_V^2+\vartheta k\partial_t\|E_\sigma^i\|_0^2+k\partial_t\|\varphi_0^{1/2}E_c^i\|_0^2+2k\|\tau^{1/2}\partial_tE_c^i\|_0^2\\
&+2k\|K^{-1/2}E_z^i\|_0^2+2k\vartheta\|\tau^{1/2}\partial_tE_\sigma^i\|_0^2+k^2\|M^{-1/2}\partial_tE_p^i\|_0^2+k^2\|\varphi_0^{1/2}\partial_tE_c^i\|_0^2\\
&+k^2\|\partial_tE_u^i\|_V^2+\vartheta k^2\|\partial_tE_\sigma^i\|_0^2=2k(M^{-1}(\dot p(t_i)-\partial_tp_i),E_p^i)\\
&+2k(\alpha\nabla\cdot(\dot{\boldsymbol{u}}(t_i)-\partial_t\boldsymbol{u}_i),E_p^i)+2k\vartheta(\tau\dot{\underline{\boldsymbol{\sigma}}}^*(t_i)-\tau\partial_t\underline{\boldsymbol{\sigma}}_i^*,\partial_tE_\sigma^i)\\
&-2k\vartheta(\varphi_1\underline{\boldsymbol{D}}\underline{\boldsymbol{\varepsilon}}(\boldsymbol{u}_i-\boldsymbol{u}_{i-1}),\partial_tE_\sigma^i)+2k(\alpha\nabla\cdot\partial_t\mathscr{E}_u(t_i),E_p^i)\\
&+2k(K^{-1}\mathscr{E}_z(t_i),E_z^i)-2k\vartheta(\varphi_1\underline{\boldsymbol{D}}\underline{\boldsymbol{\varepsilon}}(\mathscr{E}_u(t_{i-1})),\partial_tE_\sigma^i)-2k(\mathscr{E}_\sigma(t_i),\underline{\boldsymbol{\varepsilon}}(\partial_tE_u^i))\\
&-2k(\alpha\mathscr{E}_p(t_i),\nabla\cdot\partial_tE_u^i)+2k\vartheta(\varphi_1\underline{\boldsymbol{D}}\underline{\boldsymbol{\varepsilon}}(E_u^{i-1}),\partial_tE_\sigma^i)+2k(E_\sigma^i,\underline{\boldsymbol{\varepsilon}}(\partial_tE_u^i))\\
&-2k(\varphi_2E_p^{i-1},\partial_tE_c^i)+2k\tau(\dot p^*(t_i)-\partial_tp^*(t_i),\partial_tE_c^i)+2k\varphi_2(p(t_i)-p(t_{i-1}),\partial_tE_c^i).
\end{aligned}
$$

There are now fourteen terms on the right, with all except terms ten, eleven and twelve containing approximation error. This means that we will have a good deal of freedom in using kickback arguments by choosing suitable ϵ's in Young's inequality. Indeed, labelling these terms in order as I, II, III, ..., XIV we sum over $i=1,\dots,j$ and see that terms I, II, V, XII, XIII and XIV, involving E_p^i and E_c^i, can be controlled by approximation, a kickback and a Gronwall inequality. Terms III, IV and VII, involving $\partial_tE_\sigma^i$, can be dealt with by approximation and kickback while term X, due to the lagging, is easily dealt with by a Gronwall estimate. Term VI presents no difficulty but terms VIII, IX and XI will need to be summed by parts using (3).

So, to summarise, we have,

$$
\begin{aligned}
\sum_{i=1}^{j}\Big(&2k\|K^{-1/2}E_z^i\|_0^2+2k\vartheta\|\tau^{1/2}\partial_tE_\sigma^i\|_0^2+2k\|\tau^{1/2}\partial_tE_c^i\|_0^2\\
&+k^2\|M^{-1/2}\partial_tE_p^i\|_0^2+k^2\|\partial_tE_u^i\|_V^2+\vartheta k^2\|\partial_tE_\sigma^i\|_0^2+k^2\|\varphi_0^{1/2}\partial_tE_c^i\|_0^2\Big)\\
&+\|M^{-1/2}E_p^j\|_0^2+\|E_u^j\|_V^2+\vartheta\|E_\sigma^j\|_0^2+\|\varphi_0^{1/2}E_c^j\|_0^2=\sum_{i=1}^{j}\left(\mathrm{I}+\mathrm{II}+\cdots+\mathrm{XI}\right),
\end{aligned}
$$

and we now estimate the summed terms on the right in the way described above. To do this we will make use of results of the following type. Since $\dot v(t_i)-\partial_tv_i=k^{-1}\int_{t_{i-1}}^{t_i}\int_s^{t_i}\ddot v(\xi)\,d\xi ds$, it is easily deduced for a scalar product (on X say) and its norm that for all $p\geqslant 1$,

$$
\begin{aligned}
|(\dot v(t_i)-\partial_tv_i,w)| &\leqslant k^{1-1/p}\|w\|_X\,\|\ddot v\|_{L_p(t_{i-1},t_i;X)}.\\
|(v_i-v_{i-1},w)| &\leqslant k^{1-1/p}\|w\|_X\,\|\dot v\|_{L_p(t_{i-1},t_i;X)},\\
\|\partial_tv(t_i)\|_X &\leqslant k^{-1/p}\|\dot v\|_{L_p(t_{i-1},t_i;X)},
\end{aligned}
$$

where w is not time dependent.

We apply Young's inequality to terms I, II and V with $\epsilon=6$ for the j–th term in the sum

and arrive—first in detail, and then more succinctly—at,

$$\sum_{i=1}^{j}\Big|\mathrm{I}+\mathrm{II}+\mathrm{V}\Big| \leqslant \frac{1}{2}\|M^{-1/2}E_p^j\|_0^2+3k\sum_{i=1}^{j-1}\|M^{-1/2}E_p^i\|_0^2+k^2\|M^{-1/2}\ddot{p}\|^2_{L_2(0,t_{j-1};L_2(\Omega))}$$
$$+6k^3\|M^{-1/2}\ddot{p}\|^2_{L_2(t_{j-1},t_j;L_2(\Omega))}+k^2\|M^{1/2}\alpha\nabla\cdot\ddot{\boldsymbol{u}}\|^2_{L_2(0,t_{j-1};\boldsymbol{L}_2(\Omega))}$$
$$+6k^3\|M^{1/2}\alpha\nabla\cdot\ddot{\boldsymbol{u}}\|^2_{L_2(t_{j-1},t_j;\boldsymbol{L}_2(\Omega))}+t_{j-1}\|M^{1/2}\alpha\nabla\cdot\dot{\mathscr{E}}_u\|^2_{L_\infty(0,t_{j-1};\boldsymbol{L}_2(\Omega))}$$
$$+6k^2\|M^{1/2}\alpha\nabla\cdot\dot{\mathscr{E}}_u\|^2_{L_\infty(t_{j-1},t_j;\boldsymbol{L}_2(\Omega))},$$
$$\leqslant \frac{1}{2}\|M^{-1/2}E_p^j\|_0^2+3k\sum_{i=1}^{j-1}\|M^{-1/2}E_p^i\|_0^2$$
$$+Ck^2\left(\|\ddot{p}\|^2_{L_2(0,t_j;L_2(\Omega))}+\|\nabla\cdot\ddot{\boldsymbol{u}}\|^2_{L_2(0,t_j;\boldsymbol{L}_2(\Omega))}\right)+Ct_{j-1}\|\nabla\cdot\dot{\mathscr{E}}_u\|^2_{L_\infty(0,t_j;\boldsymbol{L}_2(\Omega))}.$$

Similarly, for terms III, IV and VII using $\epsilon=5$ in each Young's inequality we have,

$$\sum_{i=1}^{j}\Big|\mathrm{III}+\mathrm{IV}+\mathrm{VII}\Big| \leqslant \frac{3}{5}\vartheta k\sum_{i=1}^{j}\|\tau^{1/2}\partial_t E_\sigma^i\|_0^2+C\vartheta k^2\left(\|\ddot{\underline{\boldsymbol{\sigma}}}^*\|^2_{L_2(0,t_j;\underline{\boldsymbol{L}}_2(\Omega))}+\|\dot{\boldsymbol{u}}\|^2_{L_2(0,t_j;V)}\right)$$
$$+C\vartheta t_j\|\mathscr{E}_u\|^2_{L_\infty(0,t_j;V)},$$

while X and VI yield,

$$\sum_{i=1}^{j}\Big|\mathrm{X}+\mathrm{VI}\Big| \leqslant \frac{1}{5}\vartheta k\sum_{i=1}^{j}\|\tau^{1/2}\partial_t E_\sigma^i\|_0^2+k\sum_{i=1}^{j}\|K^{-1/2}E_z^i\|_0^2$$
$$+Ct_j\|\mathscr{E}_z\|^2_{L_\infty(0,t_j;\boldsymbol{L}_2(\Omega))}+C\vartheta k\sum_{i=1}^{j-1}\|E_u^i\|_V^2.$$

Next, for terms VIII, IX and XI we use (3) to get,

$$\sum_{i=1}^{j}\Big(\mathrm{VIII}+\mathrm{IX}+\mathrm{XI}\Big)=-2(\mathscr{E}_\sigma(t_j),\underline{\boldsymbol{\varepsilon}}(E_u^j))-2(\alpha\mathscr{E}_p(t_j),\nabla\cdot E_u^j)-2(E_\sigma^j,\underline{\boldsymbol{\varepsilon}}(E_u^j))$$
$$+2k\sum_{i=1}^{j}(\alpha\partial_t\mathscr{E}_p(t_i),\nabla\cdot E_u^{i-1})+2k\sum_{i=1}^{j}(\partial_t\mathscr{E}_\sigma(t_i),\underline{\boldsymbol{\varepsilon}}(E_u^{i-1}))-2k\sum_{i=1}^{j}(\partial_t E_\sigma^i,\underline{\boldsymbol{\varepsilon}}(E_u^{i-1}).$$

Hence, for all $\epsilon>0$, there is a $C_\star$ depending only on $\underline{\boldsymbol{D}}$ such that,

$$\sum_{i=1}^{j}\Big|\mathrm{VIII}+\mathrm{IX}+\mathrm{XI}\Big| \leqslant 3\epsilon C_\star\Big(\|\mathscr{E}_\sigma(t_j)\|_0^2+\|\alpha\mathscr{E}_p(t_j)\|_0^2\Big)+3\epsilon C_\star\|E_\sigma^j\|_0^2+\frac{1}{\epsilon}\|E_u^j\|_V^2$$
$$+\frac{\vartheta k}{5}\sum_{i=1}^{j}\|\tau^{1/2}\partial_t E_\sigma^i\|_0^2+C_\star t_j\|\dot{\mathscr{E}}_\sigma\|^2_{L_\infty(0,t_j;\underline{\boldsymbol{L}}_2(\Omega))}+C_\star t_j\|\alpha\dot{\mathscr{E}}_p\|^2_{L_\infty(0,t_j;L_2(\Omega))}$$
$$+\left(2+\frac{5C_\star}{\vartheta\tau}\right)k\|E_u^0\|_V^2+\left(2+\frac{5C_\star}{\vartheta\tau}\right)k\sum_{i=1}^{j-1}\|E_u^i\|_V^2.$$

Lastly, for terms XII, XIII and XIV we have

$$\sum_{i=1}^{j}\Big|\mathrm{XII}+\mathrm{XIII}+\mathrm{XIV}\Big| \leqslant 3\tau k^2\|\ddot{p}^*\|^2_{L_2(0,t_j;L_2(\Omega))}+\frac{3\varphi_2 k^2}{\tau}\|\dot{p}\|^2_{L_2(0,t_j;L_2(\Omega))}$$
$$+k\sum_{i=1}^{j}\|\tau^{1/2}\partial_t E_c^i\|_0^2+\frac{3\varphi_2^2 Mk}{\tau}\sum_{i=1}^{j-1}\|M^{-1/2}E_p^i\|_0^2.$$

Assembling all of these results produces,

$$\frac{1}{2}\|M^{-1/2}E_p^j\|_0^2+\left(1-\frac{1}{\epsilon}\right)\|E_u^j\|_V^2+(\vartheta-3\epsilon C_\star)\|E_\sigma^j\|_0^2+\|\varphi_0^{1/2}E_c^j\|_0^2$$
$$+\sum_{i=1}^{j}\Big(k\|K^{-1/2}E_z^i\|_0^2+k\vartheta\|\tau^{1/2}\partial_t E_\sigma^i\|_0^2+k\|\tau^{1/2}\partial_t E_c^i\|_0^2+k^2\|M^{-1/2}\partial_t E_p^i\|_0^2$$
$$+k^2\|\partial_t E_u^i\|_V^2+\vartheta k^2\|\partial_t E_\sigma^i\|_0^2+k^2\|\varphi_0^{1/2}\partial_t E_c^i\|_0^2\Big)\leqslant Ck^2\Big(\|\dot{p}\|^2_{H^1(0,t_j;L_2(\Omega))}$$
$$+\vartheta\|\dot{\boldsymbol{u}}\|^2_{L_2(0,t_j;V)}+\|\nabla\cdot\ddot{\boldsymbol{u}}\|^2_{L_2(0,t_j;\boldsymbol{L}_2(\Omega))}+\vartheta\|\ddot{\underline{\boldsymbol{\sigma}}}^*\|^2_{L_2(0,t_j;\underline{\boldsymbol{L}}_2(\Omega))}+\|\ddot{p}^*\|^2_{L_2(0,t_j;L_2(\Omega))}\Big)$$
$$+C_\star t_j\Big(\|\dot{\mathscr{E}}_\sigma\|^2_{L_\infty(0,t_j;\underline{\boldsymbol{L}}_2(\Omega))}+\|\alpha\dot{\mathscr{E}}_p\|^2_{L_\infty(0,t_j;L_2(\Omega))}\Big)+3\epsilon C_\star\Big(\|\mathscr{E}_\sigma(t_j)\|_0^2+\|\alpha\mathscr{E}_p(t_j)\|_0^2\Big)$$
$$+Ct_j\Big(\|\nabla\cdot\dot{\mathscr{E}}_u\|^2_{L_\infty(0,t_j;\boldsymbol{L}_2(\Omega))}+\vartheta\|\mathscr{E}_u\|^2_{L_\infty(0,t_j;V)}+\|\mathscr{E}_z\|^2_{L_\infty(0,t_j;\boldsymbol{L}_2(\Omega))}\Big)$$
$$+3k\left(1+\frac{\varphi_2^2 M}{\tau}\right)\sum_{i=1}^{j-1}\|M^{-1/2}E_p^i\|_0^2+\left(C\vartheta+\left(2+\frac{5C_\star}{\vartheta\tau}\right)\right)k\sum_{i=1}^{j-1}\|E_u^i\|_V^2,$$

and by choosing, for example, $\epsilon=2$ and any $\vartheta>6C_\star$ we complete the proof by using (25) and Gronwall's inequality.

Theorem 4.2 (*a priori* error bound) *Under the assumptions of Lemma 4.1 we have for the lagged scheme, and with any time step $k>0$, that*

$$\left(k\sum_{i=1}^{j}\Big(\|K^{-\frac{1}{2}}(\boldsymbol{z}(t_i)-\boldsymbol{z}_i^h)\|_0^2+\|\tau^{\frac{1}{2}}\partial_t(\underline{\boldsymbol{\sigma}}^*(t_i)-\underline{\boldsymbol{\sigma}}_i^{*h})\|_0^2+\|\varphi_0^{1/2}\partial_t(p^*(t_i)-p_i^{*h})\|_0^2\Big)\right)^{1/2}$$
$$+\|M^{-\frac{1}{2}}(p(t_j)-p_j^h)\|_0+\|\boldsymbol{u}(t_j)-\boldsymbol{u}_j^h\|_V+\|\varphi_0^{1/2}(p^*(t_j)-p_j^{*h})\|_0+\|\underline{\boldsymbol{\sigma}}^*(t_j)-\underline{\boldsymbol{\sigma}}_j^{*h}\|_0\leqslant Ck+Ch$$

for a positive constant, C, independent of h and k.

Proof. Use Lemma 4.1, the definitions of the error components, and the triangle inequality.

5 Numerical experiments

To illustrate the error bound derived in the previous section we substitute into the PDE system a simple chosen form for pressure and displacement so that we may determine exact (up to quadrature error) values of error norms. Specifically we take,

$$\begin{aligned} p &= (t+3t^4)\cos(3x)\cos(2y)\\ \text{and}\qquad \boldsymbol{u} &= (t+2t^3)\begin{pmatrix}\cos(x/3)\cos(2y)\\ \cos(2x)\cos(y/3)\end{pmatrix}\end{aligned}$$

In the absence of viscoelasticity (i.e. when $\varphi_0 = 1$) this procedure is straightforward. We just use the exact solutions in the PDE's so as to derive the corresponding forms for the data. However, when $\varphi_0 \in (0,1)$ the situation is a little more complicated and less easy to implement. The root cause is the absence of free-to-choose loads on the right hand side of the internal variable ODE's for p^* and $\underline{\boldsymbol{\sigma}}^*$. This means that the forms of these internal variables are dependent on the forms chosen for the pressure and displacement. Of course, we could introduce arbitrary loads into these ODE's but then the software becomes unnecessarily convoluted (the boundary tractions are affected and the physical meaning of p^* and $\boldsymbol{\sigma}^*$ becomes obscured). Some notes on how the exact solutions are implemented in the presence of viscoelasticity are given in Appendix A. We note also that any artificially created solution must respect the symmetry of the stress tensors, but (for simplicity) we have not taken the extra step in these artificial solutions of respecting the homogeneous boundary data assumed earlier for the theory.

Table 1: values of $\|\nabla\{\boldsymbol{u} - \boldsymbol{u}^h\}\|_{\ell_\infty(\boldsymbol{L}_2)}$ for the lagged scheme.

N	M					
	2	4	8	16	32	64
2	8.68707	4.3788	2.22349	1.19874	0.756209	0.598015
4	8.67769	4.36655	2.18775	1.12149	0.621019	0.41139
8	8.67359	4.36337	2.17547	1.09235	0.563691	0.316704
16	8.67194	4.36322	2.17239	1.08386	0.545676	0.282632
32	8.67126	4.36362	2.17187	1.08172	0.540773	0.272697
64	8.67097	4.36395	2.1719	1.08125	0.539536	0.270075

Table 2: values of $\|\{p - p^h\}\|_{\ell_\infty(L_2)}$ for the lagged scheme.

N	M					
	2	4	8	16	32	64
2	9.38953	5.08582	2.5632	1.28806	0.652707	0.342683
4	9.37828	5.08749	2.56282	1.28513	0.645799	0.328787
8	9.37091	5.08878	2.56305	1.28421	0.643256	0.32341
16	9.36674	5.08959	2.56335	1.28405	0.642536	0.321779
32	9.36452	5.09003	2.56356	1.28407	0.642371	0.321344
64	9.36338	5.09027	2.56369	1.28411	0.642345	0.321238

For these numerical experiments we consider the $d = 2$ case only (i.e. $\Omega \subset \mathbb{R}^2$) by taking $\Omega = (0,1)^2$. We let $T^h \in \{\mathscr{T}\}_h$ be a member of a family of quasiuniform and shape regular triangulations of Ω where each 'mesh' is formed by taking an $M \times M$ array of the basic building block $\boxtimes$. Thus we get $h = M^{-1}$ and $(M+1)^2 + M^2$ triangle-corner nodes for a given $M \in \mathbb{N}$. Because we are dealing here with a simple model problem we were able to carry out all of the computations in *FreeFem++ v.3.9* (see `www.freefem.org`) and solve the pressure and displacement problems simultaneously. However, in practice and for large scale simulations, we note that iterative coupling procedures are usually used, see [16] for example.

For the numerical tests that follow we used the parameter values $T = 2$, $E = 3$, $\nu = 0.3$ so that $\lambda = 1.73077$ and $\mu = 1.15385$ by the standard Hooke's law expressions $\lambda =$

Table 3: values of $\sqrt{k}\|\{K^{-1}\boldsymbol{z}^h + \nabla p\}\|_{\ell_2(\boldsymbol{L}_2)}$ for the lagged scheme.

N	M					
	2	4	8	16	32	64
2	35.9875	18.6286	9.40366	4.73244	2.4008	1.26329
4	26.8113	13.8854	7.00643	3.51898	1.7712	0.905571
8	21.997	11.3967	5.74972	2.88516	1.44684	0.729304
16	19.6008	10.158	5.12453	2.57059	1.28732	0.645383
32	18.4153	9.54512	4.81536	2.41526	1.20901	0.605083
64	17.8271	9.24103	4.66198	2.33826	1.17033	0.585439

Table 4: values of $\|\{\underline{\boldsymbol{\sigma}}^* - \underline{\boldsymbol{\sigma}}^{*h}\}\|_{\ell_\infty(\underline{\boldsymbol{L}}_2)}$ for the lagged scheme.

N	M					
	2	4	8	16	32	64
2	1.15855	1.14977	1.14785	1.14739	1.14728	1.14725
4	0.703167	0.674952	0.668198	0.666523	0.66611	0.66601
8	0.434622	0.377434	0.361973	0.358026	0.357038	0.356793
16	0.315034	0.224688	0.195174	0.18711	0.18505	0.184534
32	0.274159	0.160543	0.114026	0.0991323	0.0950754	0.0940387
64	0.262635	0.139397	0.0806262	0.0573534	0.0499373	0.0479155

$E\nu/((1+\nu)(1-2\nu))$ and $\mu = E/(2+2\nu)$. We also used $\varphi_0 = 0.5$, $\varphi_1 = 0.5$, $\tau = 10$, $\alpha = 2$, $\eta = 0.125$, $\zeta = 2.5$, $K = 4$ and $M = 2$ (which shouldn't cause any confusion with M, the grid parameter, above).

The results are shown for the lagged scheme (using $\dashv_1$) in Tables 1, 2, 3, 4 and 5 and for interest, although not covered by our error bound, for the non-lagged scheme (using $\dashv_0$) in Tables 6, 7, 8, 9 and 10. In each case we clearly see the $O(h+k)$ convergence down the diagonals.

6 A practical example

In this section we attempt to illustrate the behaviour of this model in a more realistic geomechanics setting. We start by considering a 1 km by 500 m vertical cross section of rock skeleton with Young's modulus $E = 4.0 \times 10^7$ Pa and Poisson's ratio $\nu = 0.3$. Thus $\Omega = \{0 < x < 1000 \text{ and } -500 < y < 0\}$ and we take $T = 6$, $\zeta = 2.5$, $K = 10^{-5}$, $M = 10$ and compute on a 40×20 mesh of isoceles triangles (with the diagonals flipped at the top left and bottom right corners of Ω to avoid having all of those triangles' nodes lying on $\partial\Omega$). Note that these values have been chosen for the purposes of illustration only. The discretization is otherwise exactly as described above in Section 5, and we use the lagged scheme.

For the body forces we take $\boldsymbol{f} = \boldsymbol{0}$ and for the tractions we take: $\boldsymbol{g} = (0, -1000x)$ on $y = 0$ (the top); $\boldsymbol{g} = (1000(500+y), 0)$ on $x = 0$ (the left); and, $\boldsymbol{g} = (0,0)$ on $x = 1000$ (the right). On the bottom where $y = -500$ we impose $\boldsymbol{u} = \boldsymbol{0}$. For the pressure

Table 5: values of $\|\{p^* - p^{*h}\}\|_{\ell_\infty(L_2)}$ for the lagged scheme.

N	M					
	2	4	8	16	32	64
2	0.0195518	0.0189307	0.018734	0.0186829	0.01867	0.0186668
4	0.0143455	0.0123796	0.0116986	0.0115168	0.0114706	0.011459
8	0.0113932	0.00813415	0.00679894	0.00641173	0.00631057	0.00628499
16	0.0102571	0.00622387	0.00422661	0.00353908	0.00334407	0.00329345
32	0.00989466	0.00556795	0.00315716	0.00214426	0.00180237	0.0017061
64	0.00978408	0.00537567	0.00280565	0.0015844	0.00107868	0.000909106

Table 6: values of $\|\nabla\{\boldsymbol{u} - \boldsymbol{u}^h\}\|_{\ell_\infty(\boldsymbol{L}_2)}$ for the non-lagged scheme.

N	M					
	2	4	8	16	32	64
2	8.6951	4.43003	2.30181	1.32295	0.934934	0.810744
4	8.67776	4.38106	2.20244	1.13852	0.645629	0.445535
8	8.67323	4.36934	2.17994	1.09511	0.565685	0.318684
16	8.67175	4.36609	2.17438	1.08476	0.545746	0.281899
32	8.67117	4.36505	2.17287	1.08218	0.540842	0.272391
64	8.67092	4.36467	2.17241	1.08151	0.539614	0.270011

equation we assume a simple hydrostatic pressure field and take an initial pressure of $p(x, y, 0) = -8000y$ (this approximates $\varrho g y$ for $\varrho = 800$ and $g = 9.81$). Consistent with this we set the fluxes as $\boldsymbol{z}^\flat = (0, 0)$ on the left and right; $\boldsymbol{z}^\flat = (0, 8000)$ on the top; and, $\boldsymbol{z}^\flat = (0, -8000)$ on the bottom.

To demonstrate the effect of the coupling and of the viscoelasticity on the deformation and pressure we consider the four cases corresponding to $\alpha = 1.0$ or $\alpha = 0.1$ and $\{\varphi_0, \varphi_1\} = \{1, 0\}$ or $\{\varphi_0, \varphi_1\} = \{0.8, 0.2\}$ with, in each case, $\tau = 10$ (recall that $\varphi_1 = 1 - \varphi_0$ and in some sense measures the 'amount' of viscous effect present in the material).

The deformed meshes, using a scaling of $10\boldsymbol{u}$ at the final time are shown in Figure 1 while the final pressure fields are shown in Figure 2. The shading corresponds to pressure levels increasing from $-500\,000$ to $4\,500\,000$ in steps of $500\,000$. The 'stair-casing' is an artefact of the piecewise constant pressure field. These results will be discussed in the conclusions.

7 Concluding remarks

We have presented an extension to a fully discrete mixed and Galerkin approximation to poroelasticity to allow for viscoelastic relaxation in the porous media. Our lagged numerical scheme is unconditionally stable, has optimal convergence rates and is simple to implement into an existing poroelasticity solver. A manufactured solution indicates that the lagged scheme delivers a numerical solution that is of equivalent quality as the fully coupled non-lagged scheme but is easier to implement.

Moving on now to consider the 'practical example' we can see from the left of Figure 1 that

Table 7: values of $\|\{p-p^h\}\|_{\ell_\infty(L_2)}$ for the non-lagged scheme.

N	M					
	2	4	8	16	32	64
2	9.39488	5.0868	2.56307	1.28698	0.650218	0.337752
4	9.38164	5.08822	2.56292	1.28478	0.644859	0.32682
8	9.37278	5.08923	2.56317	1.28414	0.642985	0.322802
16	9.36772	5.08983	2.56344	1.28405	0.642473	0.321615
32	9.36503	5.09016	2.56361	1.28408	0.642361	0.321304
64	9.36364	5.09033	2.56371	1.28412	0.642345	0.32123

Table 8: values of $\sqrt{k}\|\{K^{-1}\boldsymbol{z}^h+\nabla p\}\|_{\ell_2(\boldsymbol{L}_2)}$ for the non-lagged scheme.

N	M					
	2	4	8	16	32	64
2	35.9945	18.6309	9.4038	4.7308	2.39669	1.25506
4	26.8149	13.8868	7.0067	3.5185	1.76977	0.902555
8	21.9988	11.3974	5.74994	2.88508	1.44643	0.728381
16	19.6016	10.1583	5.12466	2.5706	1.28722	0.645132
32	18.4158	9.54531	4.81544	2.41528	1.209	0.605022
64	17.8274	9.24113	4.66202	2.33828	1.17033	0.585426

the relatively small amount of viscoelasticity with only small pressure coupling, $\alpha = 0.1$, has little effect on the final deformed shape of the domain. This is to be expected since the longer term creeping deformation is restricted by the long term elastic modulus, $\varphi_0 E$, and the pressure effect on the displacement equations is 'small'. However, when the coupling is increased we see from the right of Figure 1 that the presence of viscous effects has marked effect. On the other hand we observe from Figure 2 that the coupling parameter exerts no discernable influence on the final pressure field but that the presence of even this small amount of viscoelasticity has a rather profound effect.

Of course these findings are for these data only and must be taken with some caution before they can be extrapolated to 'reality'. On the other hand what we have demonstrated is that the addition to the poroelasticity equations of viscoelastic damping in the skeleton produces novel effects and gives an extra dimension of capability to the modeller — whether the concern be with rock, biotissue or indeed any other porous media comprising of a 'lossy' skeleton material.

In closing we note that further extensions to this work could include plasticity, thermal effects, nonlinearities and dynamics. It seems that the last of these could readily be included in the working given above since if $(\varrho\ddot{\boldsymbol{u}}(t), \boldsymbol{\chi})$ is included in the displacement equation then, on choosing $\boldsymbol{\chi} = \dot{\boldsymbol{u}}(t)$, we get,

$$(\varrho\ddot{\boldsymbol{u}}(t), \dot{\boldsymbol{u}}(t)) = \frac{1}{2}\frac{d}{dt}\|\varrho^{1/2}\dot{\boldsymbol{u}}(t)\|_0^2$$

which integrates to give the change in kinetic energy from 0 to t.

Table 9: values of $\|\{\underline{\boldsymbol{\sigma}}^* - \underline{\boldsymbol{\sigma}}^{*h}\}\|_{\ell_\infty(\underline{\boldsymbol{L}}_2)}$ for the non-lagged scheme.

N	M					
	2	4	8	16	32	64
2	1.5831	1.59922	1.60076	1.6015	1.60181	1.60193
4	0.773958	0.754716	0.747508	0.745866	0.745517	0.745445
8	0.436457	0.381349	0.363773	0.359373	0.358312	0.358056
16	0.31118	0.21987	0.187171	0.178202	0.17594	0.17538
32	0.272746	0.158392	0.108855	0.0926089	0.0881529	0.0870158
64	0.262407	0.139102	0.0786484	0.0540869	0.0460544	0.0438365

Table 10: values of $\|\{p^* - p^{*h}\}\|_{\ell_\infty(L_2)}$ for the non-lagged scheme.

N	M					
	2	4	8	16	32	64
2	0.0311587	0.0328927	0.033422	0.0335656	0.0336022	0.0336114
4	0.0163469	0.0154788	0.0152005	0.0151359	0.01512	0.0151161
8	0.0114287	0.00860312	0.00750266	0.00720118	0.00712384	0.00710438
16	0.0101024	0.00620275	0.00430197	0.00366838	0.00349159	0.00344595
32	0.00979528	0.00551581	0.00313387	0.00214258	0.0018106	0.00171753
64	0.00973235	0.00534539	0.00278589	0.00157134	0.00106805	0.00089906

References

[1] Hans-Dieter Alber. *Materials with memory: initial-boundary value problems for constitutive equations with internal variables*, volume 1682 of *Lecture Notes in Mathematics*. Springer-Verlag, 1998.

[2] Philip A. Allen and John R. Allen. *Basin analysis: principles and applications*. Blackwell, 1990.

[3] Norbert Bauermeister and Simon Shaw. Finite-element approximation of non-Fickian polymer diffusion. *IMA J. Numer. Anal.*, 30:702—730, 2010. doi: 10.1093/imanum/drn071; BURA: http://hdl.handle.net/2438/3113 (BICOM Tech. Rep. 08/1, see `www.brunel.ac.uk/bicom`).

[4] James Case. Recreating the great San Francisco earthquake. *SIAM News*, 42(3):1,8, April 2009. (News journal of the Society for Industrial and Applied Mathematics).

[5] H.-Y. Chen, L.W. Teufel, and R.L. Lee. Coupled fluid flow and geomechanics in reservoir study - I. theory and governing equations. Technical report, Society of Petroleum Engineers Inc., 1995. SPE 30752. Presented at SPE Annual Technical Conference and Exhibition, Dallas, USA, 22-25 October 1995.

[6] V.A. Chernykh. Nonlinear elastic filtration regime in viscoelastic porous medium. *Fluid Dynamics*, 5:310—314, 1970.

[7] O. Coussy. *Poromechanics*. John Wiley & Sons, 2004.

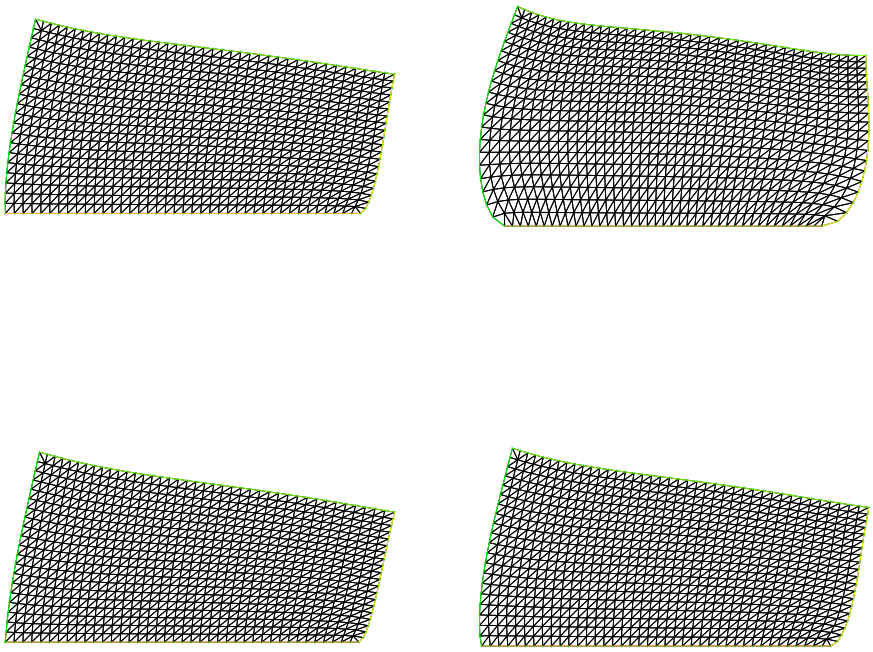

Figure 1: *Deformed meshes* (*using* $10\boldsymbol{u}$) *at* T. *Those on the left* (*right*) *correspond to* $\alpha = 0.1$ ($\alpha = 1.0$) *and those on the top* (*bottom*) *to* $\varphi_0 = 1.0$ ($\varphi_0 = 0.8$).

[8] W. Ehlers and B. Markert. On the viscoelastic behaviour of fluid saturated porous materials. *Granular Matter*, 2:153—161, 2000.

[9] Almut Eisenträger. Modelling flow of cerebrospinal fluid. Technical report, St. John's College, University of Oxford, 2009. Transfer Report.

[10] J. D. Ferry. *Viscoelastic properties of polymers*. John Wiley and Sons Inc., 1970.

[11] J. M. Golden and G. A. C. Graham. *Boundary value problems in linear viscoelasticity*. Springer-Verlag, 1988.

[12] Roderic Lakes. *Viscoelastic materials*. Cambridge University Press, New York, 2009.

[13] R. Liu, M.F. Wheeler, C.N. Dawson, and R. Dean. Modeling of convection-dominated thermoporomechanics problems using incomplete interior penalty Galerkin method. Submitted to Comp. Meth. Appl. Mech. Eng., 2009.

[14] Robert B. Lowrie. A comparison of implicit time integration methods for nonlinear relaxation and diffusion. *J. Comp. Phys.*, 196:566—590, 2004.

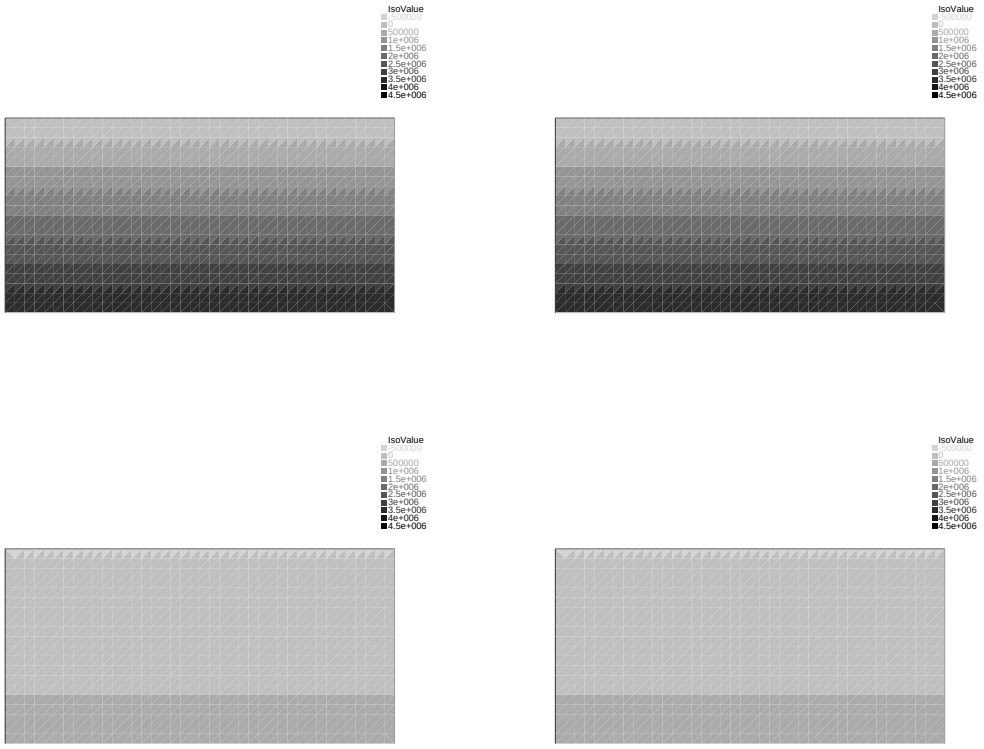

Figure 2: *A 'contour' plot of the piecewise constant pressure at T. Those on the left (right) correspond to $\alpha = 0.1$ ($\alpha = 1.0$) and those on the top (bottom) to $\varphi_0 = 1.0$ ($\varphi_0 = 0.8$).*

[15] Bernd Markert. A biphasic continuum approach for viscoelastic high-porosity foams: comprehensive theory, numerics and applications. *Arch. Comput. Methods Eng.*, 15:371—446, 2008.

[16] Andro Mikelić and Mary F. Wheeler. Convergence of iterative coupling for coupled flow and geomechanics. Submitted.

[17] Karol Miller. Constitutive model of brain tissue suitable for finite element analysis of surgical procedures. *Journal of Biomechanics*, 32:531—537, 1999.

[18] Louis Moresi, Frédéric Dufour, and Hans-Bernd Mühlhaus. Mantle convection modeling with viscoelastic/brittle lithosphere: numerical methodology and plate tectonic modeling. *Pure Appl. Geophys.*, 159:2335—2356, 2002.

[19] H. Ajabi Naeeni and M. Haghpanahi. Viscoelastic modeling of brain MRE data using FE method. *World Academy of Science, Engineering and Technology*, 54:726—729, 2009.

[20] Philip Joseph Philips and Mary F. Wheeler. A coupling of mixed and continuous Galerkin finite element methods for poroelasticity. Technical report, CSM, University of Texas at Austin, 2007. To appear in Comput. Geosci.

[21] Philip Joseph Philips and Mary F. Wheeler. A coupling of mixed and continuous Galerkin finite element methods for poroelasticity I: the continuous in time case. *Comput. Geosci.*, 11:131—144, 2007.

[22] Philip Joseph Philips and Mary F. Wheeler. A coupling of mixed and continuous Galerkin finite element methods for poroelasticity II: the discrete-in-time case. *Comput. Geosci.*, 11:145—158, 2007.

[23] P. A. Raviart and J. M. Thomas. A mixed finite element method for second order elliptic problems. Number 606 in Lecture Notes in Mathematics, pages 292—315. Springer-Verlag, Berlin, Heidelberg, 1977. Proceedings of the conference (Rome 1975) of the same name.

[24] Beatrice Riviere and Simon Shaw. Discontinuous Galerkin finite element approximation of nonlinear non-Fickian diffusion in viscoelastic polymers. *SIAM Journal on Numerical Analysis*, 44(6):2650–2670, 2006.

[25] Eduard Rohan, Simon Shaw, and John R Whiteman. Poro-viscoelasticity modelling based on upscaling quasistatic fluid-saturated solids. Technical report, BICOM, Brunel University, 2012. Technical Report 12/1, `www.brunel.ac.uk/bicom`. Submitted to *Comp. Geo.*

[26] S. Sivaloganathan, M. Stastna, G. Tenti, and J.M. Drake. A viscoelastic approach to the modelling of hydrocephalus. *Applied Mathematics and Computation*, 163:1097—1107, 2005.

[27] S. Sivaloganathan, M. Stastna, G. Tenti, and J.M. Drake. A viscoelastic model of the brain parenchyma with pulsatile ventricular pressure. *Applied Mathematics and Computation*, 165:687—698, 2005.

[28] Alan Smillie, Ian Sobey, and Zoltan Molnar. A hydroelastic model of hydrocephalus. *J. Fluid Mech.*, 539:417—443, 2005.

[29] Zeike Taylor and Karol Miller. Reassessment of brain elasticity for analysis of biomechanisms of hydrocephalus. *Journal of Biomechanics*, 37:1263—1269, 2004.

[30] Han Chou Wang and Alan S. Wineman. A mathematical model for the determination of viscoelastic behavior of brain *in vivo* — I oscillatory response. *J. Biomechanics*, 5:431—446, 1972.

[31] Changfu Wei and Kanthasamy K. Muraleetharan. Linear viscoelastic behaviour of porous media with non-uniform saturation. *Int. J. Eng. Sci.*, 45:698—715, 2007.

[32] Mary F. Wheeler and Xiuli Gai. Iteratively coupled mixed and Galerkin finite element methods for poro-elasticity. *Numer. Methods Partial Differential Equations*, 23:785—797, 2007.

[33] K.P. Wilkie, C.S. Drapaca, and S. Sivaloganathan. A theoretical study of the effect of intraventricular pulsations on the pathogenesis of hydrocephalus. *Applied Mathematics and Computation*, 215:3181—3191, 2010.

[34] Benedikt Wirth and Ian Sobey. Analytic solution during an infusion test of the linear unsteady poroelastic equations in a spherically symmetric model of the brain. *Mathematical Medicine and Biology*, 26:25—61, 2009.

[35] Benedikt Wirth, Ian Sobey, and Almut Eisenträger. A note on the solution of a poroelastic problem. Technical report, Oxford University Mathematics Institute, Numerical Analysis Group, 2010. Tech. Rep. NA 10-01.

A Notes on the exact solution

First of all let us recollect the strong form of the equations that we want to solve:

$$\begin{aligned} \frac{1}{M}\frac{\partial p}{\partial t} + \alpha\nabla\cdot\frac{\partial \boldsymbol{u}}{\partial t} - K\nabla^2 p + \eta p + \zeta p^* &= q, \\ -\nabla\cdot\underline{\boldsymbol{D}}\underline{\boldsymbol{\varepsilon}}(\boldsymbol{u}) + \nabla\cdot\underline{\boldsymbol{\sigma}}^* + \alpha\nabla p &= \boldsymbol{f}, \\ \tau\frac{\partial \underline{\boldsymbol{\sigma}}^*}{\partial t} + \underline{\boldsymbol{\sigma}}^* = \varphi_1\underline{\boldsymbol{D}}\underline{\boldsymbol{\varepsilon}}(\boldsymbol{u}), \qquad \text{and} \qquad \tau\frac{\partial p^*}{\partial t} + \varphi_0 p^* &= -\varphi_2 p, \end{aligned}$$

with zero initial data on all terms (but we allow more flexibility than in the theory on the behaviour of these test problems on the boundary of Ω). Recall also that $\underline{\boldsymbol{\sigma}} = \underline{\boldsymbol{D}}\underline{\boldsymbol{\varepsilon}}(\boldsymbol{u}) - \underline{\boldsymbol{\sigma}}^*$, $\varphi_0 > 0$, $M = (\phi\gamma + \zeta)^{-1}$ and $\eta = \zeta\varphi_1/\tau$.

To get the exact solutions that underlie the error data shown earlier we chose the forms for the pressure and displacement functions and then designed the loads and boundary conditions so that they were indeed an exact solution of the problem (this procedure is often termed the *method of manufactured solutions*).

For the viscous effects though we had to ensure that any given 'solution' did not introduce extra loads in to the right hand side of the evolution equations for the internal stress and pressure variables.

To do this we assumed first that the displacement was separable: $\boldsymbol{u}(\boldsymbol{x},t) = F_u(t)\boldsymbol{U}(\boldsymbol{x})$. Then, for the internal stress variables we have,

$$\tau\dot{\sigma}^*_{ij} + \sigma^*_{ij} = \varphi_1\lambda\delta_{ij}\nabla\cdot\boldsymbol{u} + 2\varphi_1\mu\varepsilon_{ij}(\boldsymbol{u})$$

with $\sigma^*_{ij}(\boldsymbol{x},0) = 0$. The solutions to these equations are (with the $\boldsymbol{x}$ dependence suppressed),

$$\begin{aligned} \sigma^*_{ij} &= \frac{\varphi_1}{\tau}\int_0^t e^{-(t-s)/\tau}\Big(\lambda\delta_{ij}\nabla\cdot\boldsymbol{u}(s) + 2\mu\varepsilon_{ij}(\boldsymbol{u}(s))\Big)\,ds, \\ &= \frac{\varphi_1}{\tau}\left(\frac{\lambda\delta_{ij}\nabla\cdot\boldsymbol{u}(t) + 2\mu\varepsilon_{ij}(\boldsymbol{u}(t))}{F_u(t)}\right)\int_0^t e^{-(t-s)/\tau}F_u(s)\,ds. \end{aligned}$$

The viscoelastic effect is then (for the purposes of clean coding) captured in the integral. If we take the case where $F_u(t) = t + A_u t^m$, for some constant A_u and with m a non-negative integer that we can choose, then by recursion,

$$I_m := \int_0^t e^{s/\tau}s^m\,ds \quad\Longrightarrow\quad \begin{cases} I_0 &:= \tau(e^{t/\tau} - 1), \\ I_m &:= \tau e^{t/\tau}t^m - \tau m I_{m-1}, \\ & \quad \text{for } m \geqslant 1. \end{cases}$$

Therefore, with this limited degree of flexibility for choosing the exact form of the displacements, the internal stress variables are given explicitly by,

$$\begin{pmatrix} \sigma_{11}^* \\ \sigma_{22}^* \\ \sigma_{12}^* \end{pmatrix} = \frac{\varphi_1 e^{-t/\tau}(I_1 + A_u I_m)}{\tau F_u(t)} \begin{pmatrix} \lambda\left(\frac{\partial u_1}{\partial x_1}(t) + \frac{\partial u_2}{\partial x_2}(t)\right) + 2\mu\frac{\partial u_1}{\partial x_1}(t) \\ \lambda\left(\frac{\partial u_1}{\partial x_1}(t) + \frac{\partial u_2}{\partial x_2}(t)\right) + 2\mu\frac{\partial u_2}{\partial x_2}(t) \\ \mu\left(\frac{\partial u_1}{\partial x_2}(t) + \frac{\partial u_2}{\partial x_1}(t)\right) \end{pmatrix}.$$

This is the form that was hard-coded in to the software in order to demonstrate the convergence rates.

A similar situation arises with the internal pressure variable. In this case we use the ansatz $p = P(\boldsymbol{x})F_p(t)$ and get,

$$p^*(t) = -\frac{\varphi_0\varphi_1}{\tau^2} P(\boldsymbol{x}) e^{-t/\tau'} \int_0^t e^{s/\tau'} F_p(s)\, ds$$

where $\tau' := \tau/\varphi_0$ for convenience. Taking $F_p(t) = t + A_p t^m$, where A_p is a constant and m is a non-negative integer that we can choose (not necessarily the same as the one above), we calculate that $p^*(t) = -\tau^{-2}\varphi_0\varphi_1 P(\boldsymbol{x}) e^{-t/\tau'}(I_1' + A_p I_m')$ where I_m' is identical to I_m except that it uses τ' rather than τ.

These somewhat artificial manipulations allow the construction of test problems with known exact solutions which can then be used to demonstrate the theoretical convergence rates.